# INTRODUCTION

In 1966, Dr. Andreas Rett described a neurological disorder in young severely disabled girls relentlessly wringing their hands after a period of seemingly normal early development (Rett 1966). Only 17 years later, Rett syndrome (RTT) became recognized when Hagberg and colleagues increased the worldwide awareness of the disorder in the English medical literature in 1983 with a further description of the condition of 35 girls with strikingly similar clinical features of “progressive autism, loss of purposeful hand movements, ataxia and acquired microcephaly” (Hagberg et al. 1983).

RTT is now recognized as a severe post-natal neurodevelopment disorder occurring typically in girls with a prevalence of 1:10.000-15.000 born females. It is the second cause of mental retardation in females after Down’s syndrome.

## NATURAL HISTORY OF RETT SYNDROME

RTT is a unique neurological disorder with the onset of hypotonia, autistic tendency, and abnormalities of fine finger movements and gross movements of the arms in early infancy. RTT was originally assumed to be a progressive disorder since RTT children appear to be normal for the first 6 to 18 months, with regression occurring during the course of the disease process, from late infancy to early childhood. Clinical features include specific age-dependent symptoms (Hagberg et al. 2002; figure 1). However, clinical observations have shown that the affected children are not completely normal from very early infancy (Nomura et al. 1984; Nomura & Segawa 1990) and that the clinical status of some older patients becomes static. A degenerative process in the central nervous system was suspected but

neuropathologic studies have not revealed any signs of neurodegeneration (Jellinger & Seitelberger 1986; Armstrong et al. 1995).

## AGE-RELATED ALTERATION OF SYMPTOMS

### *Early infancy (first 6 months)*

It is generally accepted that children with RTT appear normal in the initial 6 to 18 months of life. However, the analysis of motor milestones has revealed that most patients showed delays in rolling over and in head control (Nomura & Segawa 1990). A retrospective questionnaire on the behavioural characteristics in infancy showed the babies to be quiet and placid. The placidity was attributed to the decrease in postural muscle tone. The delay in decrement of daytime sleep in late infancy to early childhood was also obvious. Researchers also reported some difficulty in appearance, posture, movement, and contact.

### *Late infancy to early childhood*

Originally, late infancy to early childhood was the period believed to be associated with the onset of the classic form of RTT. This is the regression period and babies who appeared to be normal show a rather sudden onset of autistic tendency (Witt Engerstrom 1992 a and b). Delay in motor milestones becomes apparent within months, as speech delay. The loss of purposeful hand use is observed at around 12 to 18 months and is followed by pathognomonic hand stereotypies. After the occurrence of the stereotyped movements, some patients lost the ability to use words that they had previously attained, and other signs of regression become apparent.

### *Childhood to adulthood*

Autistic features begin to disappear, and the child begins to associate with the environment. However, intellectual ability is severely affected. Motor symptoms seem to show slow progression. Dystonic muscle hypertonus increases, resulting in joint contracture. Scoliosis begins to slowly progress. Abnormal autonomic function, including breathing abnormalities, becomes evident. Epileptic seizures occur in some cases. However, during this period, the patient's overall condition typically stabilizes. The severity score seems to rise until 15 years of age and to flatten at 25 years (Nomura & Segawa 2005).

*Late adulthood to old age*

In most cases, once a patient reaches adulthood, the condition stabilizes. If disease progresses, muscle tone shows plastic rigidity and parkinsonism (but without tremor) seems to present. The scoliosis can stabilize in some cases. Often epileptic seizures decrease in frequency and severity. Overall clinical features become static.

The diagnostic criteria that had initially been determined in 2002 (Hagberg et al. 2002) were simplified by Neul et al. in 2010. The necessary criteria were limitied to the presence of regression plus four main criteria. The first period of regression is followed by recovery or stabilization (typical or atypical RTT). To diagnose classic RTT all the four main criteria must be met: (i) partial or complete loss of acquired purposeful hand skills; (ii) partial or complete loss of acquired spoken language; (iii) gait abnormalities: impaired or absence of ability; (iiii) stereotypic hand movements such as hand wringing/squeezing, clapping/tapping, mouthing and washing/rubbing automatisms. The supportive criteria are not required. For the diagnosis of atypical RTT are necessary at least two of the four main criteria, and at least 5 of 11 supportive criteria: breathing disturbances when awake, bruxism when awake, impaired sleep pattern, abnormal muscle tone, peripheral vasomotor disturbances, scoliosis/kyphosis, growth retardation, small cold hands and feet, inappropriate laughing/screaming spells, diminished response to pain and intense eye communication “eye pointing”.

The atypical forms of RTT are divided into five classes: atypical variant, forme fruste, congenital, early seizure, preserved speech variant. These variants can be milder or more severe than classical RTT. Milder variants include the forme fruste and conserved speech, in which girls do not undergo the neurodevelopmental regression until 1 to 3 years of age and hand use is usually preserved. The more severe forms are the congenital form and the early-onset seizure variant that is characterized by the lack of an early period of apparently normal development and by a precocious onset of epileptic seizures (Hanefeld 1985). Approximately 83% of RTT patients are affected by the classic form, while the rest are classified as having one of the atypical forms (Kerr et al. 2001).

Given the complexity of the clinical picture associated with RTT and the difficulties in understanding the molecular pathogenesis of the disease, there is no effective cure for this disorder yet. The medical management of RTT is essentially symptomatic and

supportive and should include psychosocial support for the families, development of an appropriate education plan and assessment of available community resources. Pharmacological treatment of RTT usually includes: anticonvulsant medications, such as carbamazepine or valproic acid; L-carnitine, which may lead to an improvement of the patient's wellbeing and quality of life (Ellaway et al. 2001); naltrexone to stabilize breathing abnormalities and levodopa to alleviate muscle stiffness; magnesium to reduce the episodes of hyperventilation (Egger et al. 1992) and melatonin to improve sleep dysfunctions. Besides the pharmacological cure, RTT girls need physical therapy to improve equilibrium, to maintain flexibility and muscle strength; speech therapy to stimulate their communicative abilities and to promote interpersonal interaction (Budden et al. 1995). Moreover, diet and caloric intake in RTT patients should also be monitored to ameliorate constipation and gastrointestinal troubles (Budden et al. 1997).

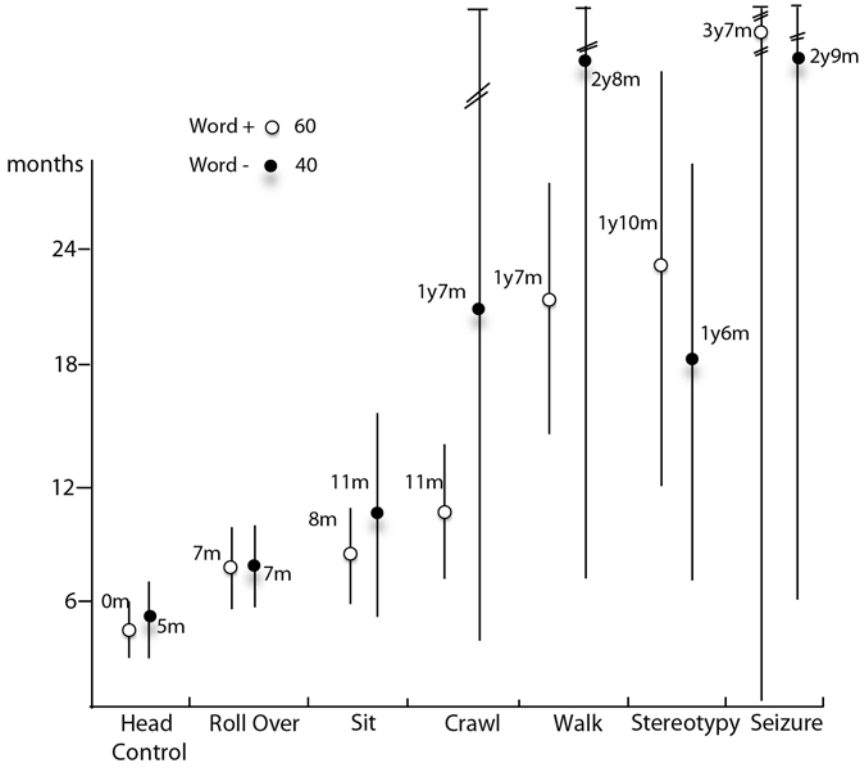


**FIGURE 1. Differences of the ages at which motor milestones were attained and onset of stereotypy and seizures in the patient groups with or without words.** The analysis was done with an increased number of patients (n=100, 60 with words and 40 without). The numbers represent the average age of onset of symptoms. (modified from Nomura & Segawa 2005).

## GENETIC BASIS OF RTT

The early observation that Rett syndrome occurred exclusively in females led to the hypothesis that it was caused by a dominant X-linked mutation that was lethal in hemizygous males (Hagberg et al. 1983). The fact that 99% of RTT cases are sporadic, the rarity of familial cases, and the small size of the affected families made conventional linkage analysis difficult, but by exclusion mapping Xq28 was identified as the candidate region (Sirianni et al. 1998; Webb et al. 1998; Xiang et al. 1998). Using a systematic gene screening approach, mutations in the gene *MECP2* encoding the X-linked methyl-CpG-binding protein 2 (MeCP2) have been identified in patients with RTT (Amir et al. 1999). Mutations in *MECP2* are found in more than 95% of classic RTT cases; most arise *de novo* in the paternal germline and often involve C to T transition at CpG dinucleotides. The spectrum of mutation types includes missense, nonsense or frameshift mutations, with over 300 unique pathogenic nucleotide changes described (Christodoulou et al. 2003), as well as deletions encompassing whole exons (Archer et al. 2006). Eight missense and nonsense mutations account for about 70% of all mutations, while small C-terminal deletions account for another 10%, and complex rearrangements constitute 6%.

## *MECP2*, A MEMBER OF THE MBD FAMILY

The *MECP2* gene is located at q28 on the human X-chromosome and has been demonstrated to undergo X inactivation in mice and humans (Adler et al. 1995). MeCP2 is a multi-domain protein, containing the founding member of the methyl-CpG-binding domain. The protein is chromatin associated and in murine cells stains with highly methylated perincentromeric heterochromatic DNA. *MECP2* consists of four exons that code for two different isoforms of the protein due to alternative splicing of exon 2 (figure 2A). The MeCP2 splice variants differ only in their N-termini; the more abundant MeCP2-e1 isoform contains 24 amino acids encoded by exon 1 and lacks the 9 amino acid encoded by exon 2, whereas the start site for the MeCP2-e2 is in exon 2 (Dragich et al. 2007; figure 2B). The MeCP2 polypeptide contains a methyl-binding domain (MBD), a transcriptional repression domain (TRD), two putative nuclear localization signals (NLS), and a WW-domain binding region at the very C-terminal tail of the protein. The MBD consists of an 85 amino acid stretch at the N-terminal end of the protein, which is both necessary and sufficient for binding to

DNA containing at least one symmetrically methylated CpG dinucleotide (Klose et al. 2005). The TRD is involved in the repressor function of MeCP2. Nan et al. described MeCP2 in 1997 as a transcriptional repressor whose potency depends on the density (about one methyl-CpG per 100 bp), and location of methyl-CpGs near a promoter. The authors demonstrated that the repressive functions of MeCP2 work also in absence of chromatin and that the TRD maintains its functions when artificially recruited to DNA by another DNA-binding domain. The mechanism by which MeCP2 represses transcription is well illuminated by its protein interactors that in general work as co-repressors and include Sin3A and histone deacetylases (HDACs; Jones at al. 1998; Nan et al. 1998) 1 and 2, the Brm SWI/SNF complex (Harikrishnan et al. 2005), the DNA methyltransferase DNMT1, the histone methyltransferase Suv39H1, c-Ski, N-CoR, LANA, and theSWI2/SNF2 DNA helicase/ATPase responsible for α-thalassemia/mental retardation syndrome X-linked (ATRX; Chahrour & Zoghbi 2007). Moreover, the transcription factors TFIIB and Pu.1 have been found associated with MeCP2. All together these data indicate that MeCP2 is able to repress gene expression through the recruitment of chromatin modifying factors. Additionally however, the repressive functions of MeCP2 have also been associated with the capacity of the protein to compact nucleosomal arrays in the absence of other proteins (Nikitina et al. 2007).

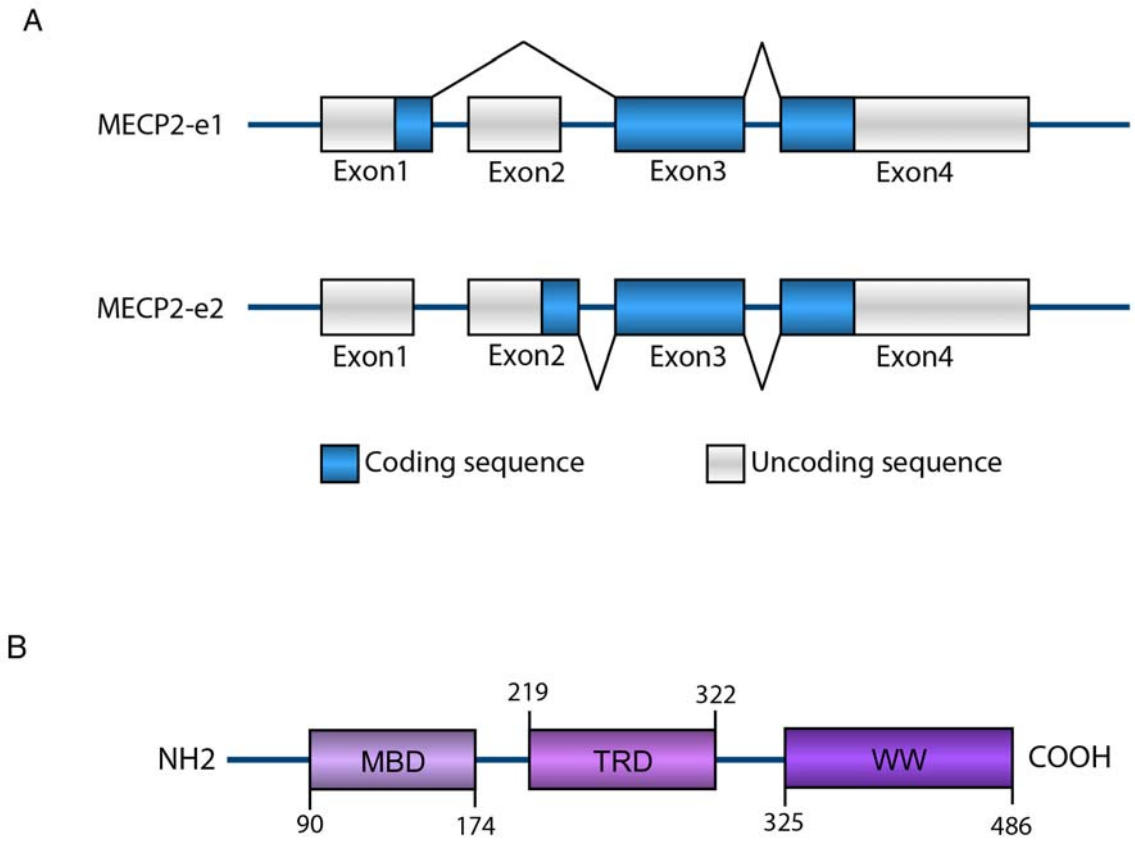


**FIGURE 2. MECP2 Gene Structure. A** Alternative splicing of the MECP2-e1 transcript excludes exon2, while the MECP2-e2 isoform is expressed from an ATG in exon 2. **B** Functional domains in the MeCP2-e2 protein sequence (modified from Weaving et al. 2005).

## PHENOTYPIC VARIABILITY IN RTT

A major source of the phenotypic variability associated with different *MECP2* mutations in females is the pattern of X chromosome inactivation (XCI). In fact, most of RTT patients are heterozygous females who can be considered mosaics of cells expressing either the normal or the mutated *MECP2* allele. Because of favourable or unfavourable XCI, different RTT girls carrying the same *MECP2* mutation can manifest a severe or a mild-to-asymptomatic phenotype.

In the past few years, more than 2,000 mutations have been reported in females with RTT. There are eight common mutations, which arise at CpG hotspots and result in loss of function due to truncated, unstable or abnormally folded proteins. More recently, large rearrangements that involve *MECP2*, including deletions, were reported in a significant proportion of patients with RTT. Altogether, *MECP2*

abnormalities might account for more than 95% of sporadic cases of classical RTT in females. The establishment of a genotype-phenotype correlation in females has been difficult and is not clear yet. However, in general, missense mutations are milder than nonsense mutations, mutations in the methyl-binding domain are often more severe than those in the transcription repression domain. More specifically, the Arg270X mutation, which is predicted to result in a truncated protein, is associated with increased mortality and, on the contrary, patients with the R133C substitution usually have a more favourable prognosis (Weaving et al. 2005). However, as missense and late-truncating mutations can lead to either classical or atypical RTT, it has been suggested that genetic background and/or non-random X-chromosome inactivation in the brain influences the biological consequences of mutations in *MECP2*. Moreover, extreme skewing of X-inactivation might account for the existence of rare female carriers with no RTT symptoms. In fact, it was entirely unanticipated to find that the mothers of some patients are heterozygous for the mutation, while having a normal intellect and no evident neurological symptoms. The finding of a *MECP2* mutation in an asymptomatic female further confirms that it is essential to look for mutations in the mothers of all patients with MECP2 mutations (Dayer et al. 2007).

## INSIGHTS INTO THE RTT PATHOGENESIS: THE MOUSE MODELS

Generation and characterization of mouse models that recapitulate the symptoms found in patients often are very useful to unveil the pathogenesis of a disease. Until 2010, there were three *Mecp2* mouse models and all of them showed a phenotype overlapping that of RTT patients. The first to be created was a conditional knockout (*Mecp2*$^{-/y}$) in which exon 3 of MeCP2 was deleted by an ubiuquitously expressed Cre-recombinase (Chen et al. 2001). Concomitantly, another mouse model, that lacks both exon 3 and 4, was generated resulting in the general loss of MeCP2 (Guy et al. 2001). Phenotypically speaking, these mice are very similar: after a period of apparently normal development (three to six weeks), the *Mecp2*$^{-/y}$ mouse develops severe and progressive neurological dysfunctions, epileptic crisis, tremors, breathing abnormalities, ataxia and die within 10 weeks of age. The phenotype in heterozygous females is less severe: they look normal even in early adulthood when, at the age of about 6 months, they start to show mild neurological alterations. It is noteworthy that, the mouse with an *Mecp2* deletion only in neurons display symptoms similar to the

ubiquitous knockout mouse, indicating that the lack of neuronal MeCP2 is sufficient to cause RTT (Chen et al. 2001). In line with this, it has been demonstrated that the expression of *Mecp2* in postmitotic neurons is sufficient to rescue the neurological phenotype in *Mecp2*-null mice (Luikenhuis et al. 2004).

As a number of RTT mutations are due to the premature truncation of the C-terminal tail of the protein, Shahbazian and colleagues generated a mouse expressing a truncated MeCP2 protein at amino acid 308 (*Mecp2*$^{308/Y}$). These mice start to develop a progressive neurological syndrome at 6 weeks of age, characterized by stereotypies, social behaviour abnormalities, seizures, motor dysfunctions, learning and memory deficit and an increased anxiety-related behaviour. Interestingly, if compared to the mice that express no MeCP2 at all (*Mecp2*$^{-/y}$), the *Mecp2*$^{308/Y}$ mice clearly display a less severe phenotype, and, accordingly, their lifespan is long and almost comparable to that of wild type animals (Shahbazian et al. 2002).

Several cases of RTT patients with the gene duplication have been reported. A mouse model (*MECP2*$^{Tg}$) overexpressing human MeCP2 at about twice the levels of the endogenous protein was generated in Zoghbi's laboratory in 2004 (Collins et al. 2004). In the first stages of life, the *MECP2*$^{Tg}$ mice show increased learning ability and synaptic plasticity. However, at 10-12 weeks of age they start to undergo a progressive neurological phenotype characterized by hypoactivity, stereotypies such as forepaw clasping, anxiety, kyphosis, epileptic crisis that become more frequent around 12 months of age when they prematurely die. Accordingly, also the overexpression of MeCP2 in postmitotic neurons has been shown to be detrimental. Therefore, this transgenic mouse model of RTT stresses the importance of a tight regulation of MeCP2 levels for a physiological neuronal functioning.

The fact that the neuropathology in RTT patients and mouse models is rather mild with no signs of severe neuronal degeneration made it intriguing to analyze whether the symptoms might be reversible upon the restoration of normal MeCP2 functions. A mouse model, in which the endogenous *Mecp2* gene was silenced by the insertion of a lox-Stop cassette that could be removed by tamoxifen induction of a Cre-recombinase fused to a modified estrogen receptor, demonstrated that advanced RTT symptoms can be reversed (Guy et al. 2007).

It remains unknown whether providing MeCP2 function exclusively during early post-natal life might be sufficient to prevent or mitigate disease in adult animals. To address this question, an adult onset model of RTT was generated in which MeCP2

removal was induced with tamoxifen at post-natal day 60 (McGraw et al. 2011). These adult knock out mice (AKO) develop symptoms of disease and behavioural deficits similar to germline null (KO) mice. By 10 weeks after dosing tamoxifen given daily to reduce whole-brain MeCP2 levels, AKO mice are less active, have abnormal gait, and develop hind-limb clasping, similar to 10-11 week-old KO mice. AKO mice also develop motor abnormalities and impaired nesting ability, as observed in KO mice. In addition, AKO and KO mice show impaired learning and memory. The expression of some genes has been investigated, and the authors found that all the genes (around 10 genes) are significantly altered in AKO animals. Lastly, both AKO and KO mice died prematurely with similar median time around 13 weeks. Taken together these results decisively show the dependence of the mature brain on MeCP2 function suggesting that therapies for RTT must be continuously maintained.

**PHOSPHORYLATION OF MeCP2 REGULATES ITS FUNCTIONS**

MeCP2 binds to methylated DNA and has been considered as a classic epigenetic factor that regulates gene expression. The revelation that it undergoes dynamic phosphorylation/dephosphorylation at multiple sites upon neuronal activity suggests that multiple signalling pathways regulate MeCP2 functions. In the nervous system, MeCP2 phosphorylation was shown to be influenced by extracellular stimuli and to dynamically regulate gene expression. In particular, MeCP2 represses the *Bdnf* promoter III and IV in rat and mouse brain, respectively, mediating its transcriptional repression. Neuronal activity causes MeCP2 phosphorylation at serine (Ser) 421 through a CamKII-dependent mechanism leading to the release of MeCP2 from the *Bdnf* promoter and the concomitantly increase of *Bdnf* transcription (Chen et al. 2003). Ser 421 phosphorylation has also been shown to be important for the capacity of MeCP2 to regulate dendritic growth and spine maturation (Zhou et al. 2006). The implication of the calcium/calmodulin-dependent protein kinase II (CamKII) in the regulation of MeCP2 function is intriguing in the context of the cognitive deficits observe in RTT since CamKII is known to play a crucial role in regulating synaptic development and plasticity.

As opposed to the activity dependent phosphorylation of Ser 421, Ser 80 was found, by Tao et al., to be constitutively phosphorylated in resting neurons and dephosphorylated upon neuronal activity (Tao et al. 2009). Interestingly, *Mecp2*$^{S80A}$-

knock-in provide the first in vivo evidence that Ser 80 and/or phosphorylation of Ser 80 has important neurobiological functions as indicated by the significant reduction of locomotor activities. Dephosphorylation of Ser 80 was found to contribute to the attenuated association of MeCP2 with some of its target chromatin regions. The opposite regulation of Ser 80 and Ser 421 phosphorylation by neuronal activity suggests that Ser 80 phosphorylation is primarily associated with MeCP2 function in resting neurons, whereas Ser 421 phosphorylation is associated with that in depolarized neurons. As show in figure 3, when a neuron transits between resting and activated states in functioning neuronal circuits, its gene transcription program also shifts between these two states. Activity dependent regulation of MeCP2 phosphorylation might be part of the switch mechanism controlling such transitions. Ser 80 phosphorylation may allow MeCP2 to rebind to chromatin when cells enter the resting state, whereas Ser 421 phosphorylation allows MeCP2 to dissociate from chromatin when cells are depolarized. The studies by Tao and colleagues, reveal another layer of complexity in fine-tuning MeCP2 function. The interplay between specific phosphorylation sites of MeCP2 orchestrates its response to changes in the sate of neuronal activity and the transcription of certain genes. This latest insight about the post-translational regulation of MeCP2 activity opens a potential therapeutic avenue to restore balanced neuronal activity in MeCP2-related disorders by targeting the associated phosphatases and kinases. Whereas CamKII has been implicated in Ser 421 phosphoryation, the homeodomain-interacting protein kinase 2 (HIPK2) was found to associate with MeCP2 *in vivo* and capable of phosphorylating Ser 80 *in vitro* and in neurons (Bracaglia et al. 2009). HIPK2 regulates cell growth and apoptosis in response to genotoxic stress (Calzado et al. 2007; Rinaldo et al. 2007) and, interestingly, the overexpression of the MeCP2 and HIPK2 either alone or together increased cell death. The implications of these studies for Rett syndrome still need to be revealed but it is relevant to mention that Hipk2-null mice have motor deficits.

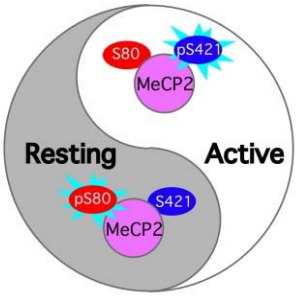


**FIGURE 3. MeCP2 phosphorylation: a balancing act in neurons.** MeCP2 in resting neurons is predominately phosphorylated at Ser 80 (pS80) and dephosphorylated at Ser 421, whereas in active neurons the protein is predominately dephosphorylated at Ser 80 and phosphorylated at Ser 421 (pS421; modified from Chao & Zoghbi 2009).

## CONSEQUENCES OF MUTATIONS IN THE KINASE CDKL5

In accordance with the evidence that the phosphorylation of MeCP2 is important in the onset of the RTT syndrome, in the 2005 Mari et al. demonstrated that the phosphorylation of MeCP2 is mediated from cyclin-dependent kinase like 5 (CDKL5). In the last six years, a number of different mutations in *CDKL5* have been reported in girls affected by a severe RTT variant, the so-called Hanefeld variant.

The frequency of CDKL5 mutations has been estimated to be about 9% in females with early onset seizures, and 28% in females with early onset seizures and infantile spasms (Nemos et al. 2009). Most mutations are identified in single cases, but some recurrent mutations are reported. Mutations in females are found all over the coding sequence of the CDKL5 gene. More than 50% of the pathogenic mutations identified so fare, reside in the catalytic domain encoding part of the gene and influence the enzymatic activity of the CDKL5 protein, suggesting that the kinase activity is required for a normal neurodevelopment. In 2004, Tao and colleagues identified three girls carrying mutations in CDKL5 and associated, for the first time, CDKL5 defects with the Hanefeld variant. The first mutation is a c.455G→T nucleotide exchange generating a cytosine-to-phenylalanine substitution of aa 152 (p.C152F); this mutation was reported to cause intractable seizures appearing at 5 weeks of age associated with mental retardation and reduced head size. The other two patients, carrying a missense mutation in aa 175 (p.R175S) were female twins. Their diagnosis was very similar: infantile spasms at tenth week of age, psychomotor retardation, stereotypic hand movements, and breathing dysfunction (Tao et al. 2004).

Concomitantly, another group identified in two monozygous female twins a deletion of nucleotide 183 (c.183delT), causing a precocious protein truncation at aa 75 (Weaving et al. 2004). In this case, the patients had rather different symptoms: whereas the first exhibited an autistic disorder without seizures, the second had severe mental retardation with infantile spasms. Analysis of the XCI did not reveal a significant difference that could be responsible for the different phenotype in the two genetically identical girls, underlying a crucial role for epigenetic or environmental events in the final phenotypic outcome of the same genetic defect. In contrast, their brother carrying the same CDKL5 mutation had a more severe pathological course until his death at 16 years of age resulting from respiratory dysfunctions.

The number of mutations have been found exclusively in the catalytic domain of the protein (A40V, R65Q, I72N, H127P, C152F, R175S, P180L, L220P, L227P), whereas single base pair substitutions at splice site closted to the intron-exon junctions leading to whole exon skipping, deletion or insertion of one more base pairs causing frameshift mutations and premature truncations of the protein (i.e. R55fsX74, T281fsX283, R781fsX783, Q834X, E879fsX908) occur anywhere in the primary structure (Scala et al. 2005; Archer et al. 2006; Mari et al. 2005; Nectoux et al. 2006). Also point mutations in the promoter, in the non coding sequence in exon 1 or within an intronic sequence have been associated with the Hanefeld variant (Evans et al. 2005). No mutations have been found in classical RTT cases indicating only a partial overlap between the phenotypes caused by CDKL5 and MeCP2 mutations. On the contrary, in the 10 years following its discovery, CDKL5 has been associated with a number of neurological and neurodevelopmental disorders other than RTT. In the 2000 a 136kb deletion spanning three different genes was found in a male patient affected by X-linked retinoschisis (XLRS; Huopaniemi et al. 2000), it was likely that the epileptic phenotype was due to the deletion of the C-terminal tail of the kinase. Later, in 2003, Kalscheuer and colleagues found *de novo* balanced X; autosome translocations, both disrupting the CDKL5 gene, in two girls affected by West syndrome (WS; Kalscheuer et al. 2003). It is characterized by the early onset of generalized epileptic seizures, hypsarrhythmia and severe to profound mental retardation.

Bienvenu's group tried to define some key clinical features in order to delineate more thoroughly the natural history of the disease (Bahi-Buisson et al. 2008). Early epilepsy, with very frequent seizures, was the main clinical characteristic in

accordance with the previous observations. The patients were also found to exhibit a normal EEG pattern, severe hypotonia, poor eye contact. In most cases, infantile spasm, some RTT-like features, such as secondary deceleration of head growth, severe motor impairment, sleep disturbance, hand apraxia, and hand stereotypes, are reported as main features associated with CDKL5 mutations (Bahi-Buisson et al. 2008; Archer et al. 2006; Grosso et al. 2007; Kalscheuer et al. 2003; Mari et al. 2005; Scala et al. 2005; Tao et al. 2004; Weaving et al. 2004). Evaluation of motor delay in CDKL5 mutation patients, indicates that all girls are severely delayed, with very limited autonomy. However, according to their ambulatory ability, two groups seem to emerge. CDKL5 mutation patients who did not acquire ambulation seem to have more severe microcephaly, hand apraxia, scarce eye communication, bruxism and sleep disturbances. Conversely, the patients who are able to walk seem to have a better eye gaze, hand use, less bruxism, and sleep disturbance. However, the prevalence of refractory epilepsy and hand stereotypies are comparable between the two groups. Several hypotheses could be proposed to explain the phenotypic heterogeneity observed in females carrying a CDKL5 mutation: (i) the nature and the location of the CDKL5 mutation; (ii) the pattern of X-chromosome inactivation; (iii) differences in the molecular and cellular consequences of the mutations. CDKL5 has also been associated with cases of West syndrome, also called X-linked infantile spasms (ISSX) when the X chromosome is involved. The involvement of CDKL5 in this pathology was identified in two unrelated girls with a pathological phenotype characterized by seizures, hypsarrhythmia and a general developmental arrest (Kalscheuer et al. 2003). West syndrome is commonly caused by mutations in the X-linked *aristaless* related box (ARX), a gene involved in neuronal embryogenesis, and by trisomy of chromosome 21 (Down's syndrome).

The rather limited number of patients described today limits the possibility of stabilizing whether a genetype-phenotype correlation exists. However, the location of mutations in the catalytic domain of CDKL5 has been suggested to be associated with earlier onset intractable infantile spasms and more severe late onset multifocal and myoclonic epilepsy than a C-terminal location of the mutation (Bahi-Buisson et al. 2008). Bahi-Buisson and colleagues analyzed the epilepsy course in 13 cases of patients with CDKL5 mutations associated with encephalopathy. This led to the description of three successive stages: *stage 1* early epilepsy (onset 1-10 weeks) with normal electroencephalogram (EEG) despite frequent convulsive seizures; *stage*

*II* epileptic encephalopathy with infantile spasms and hypsarrhythmia; *stage III* refractory epilepsy with tonic seizures and myoclonia. A late truncation was very recently linked with an exceptionally mild epilepsy phenotype (Psoni et al. 2010). However, the epilepsy phenotype may be modified by many factors as indicated by the finding that a single point mutation in exon 4 of *CDKL5* can be associated with different types of epilepsy in different individuals (Nemos et al. 2009).

## CDKL5 CHARACTERIZATION AND FUNCTIONS

The *CDKL5* gene, structured in 21 exons, encodes a protein of 1030 amino acids. A catalytic domain in the N-terminal region, spanning amino acids (aa) 13 to 297, and a long C-terminal tail characterize the primary protein structure. The catalytic domain is organized in two functional sites. The first, between aa 14 and 47, is a specific serine/threonine kinase domain and is characterized by a lysine residue (K42) localized in a glycine-rich stretch which is required for ATP binding. The second site (aa 127 to 144) is a kinase active site in which an aspartic acid (D136) is essential for the catalytic activity. In addition, CDKL5 has a Thr-Xaa-Tyr (TEY) motif corresponding to residues 169-171 resembling the dual phosphorylation site required for the activation of the mitogen-activated protein kinases (MAPK). The phosphorylation of the threonine and tyrosine residues of this motif is requested for the MAPK family members to be activated. The large C-terminal region, situated between aa 298-1030, does not share any homology with other proteins rendering the functional role of this domain difficult to predict. In this large C-terminal tail an inspection of the primary structure revealed the presence of a stretch of amino acids from 836 to 845 (LKSLRKLLHL) sharing high homology with the consensus NES (nuclear export signal; Rusconi et al. 2008).

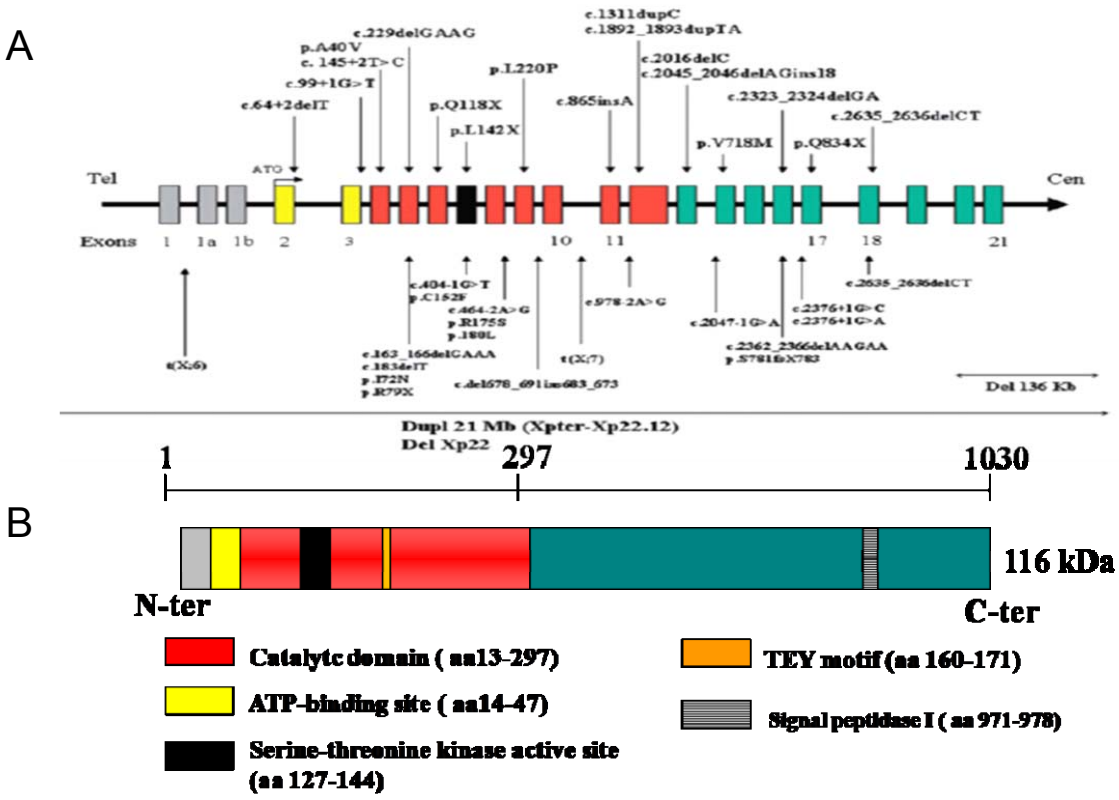


**FIGURE 4. Structure of the CDKL5 gene. A** Pathogenic mutations identified so far. **B** Schematic representation of the functional domains of the protein (modified from Bahi-Buisson et al. 2008).

The expression in mouse tissues of the *Cdkl5* gene, that shares 90% of identity at the nucleotide level to the human gene, has been extensively analysed. *Cdkl5* is expressed in several tissues, such as heart, liver, spleen, kidney and brain (Montini et al. 1998), and a smaller but abundant transcript, probably an alternative splice variant of *Cdkl5*, is also present in testis. The results obtained in mice are also true for adult human tissues but, in mice, *Cdkl5* expression peaks in spleen whereas, in human, *CDKL5* reaches its highest expression in the brain. In the adult mouse brain, *Cdkl5* is transcribed in the olfactory bulbs, cerebral cortex, cerebellum, hippocampus and dentate gyrus, basal ganglia and thalamus (Weaving et al. 2004). By in situ hybridization, no signal corresponding to *Cdkl5* RNA is detectable in early embryonic stages, from E10.5 to E17 (Montini et al. 1998) as is the case also regarding the protein expression (Rusconi et al. 2008). However, a weak staining starts to appear in the last days of embryonic development (Mari et al. 2005; Rusconi et al. 2008) and soon after birth, CDKL5 expression is strongly upregulated and reaches a plateau at

post-natal day 10 (P10). At the cellular level, CDKL5 is detected in all mature NeuN-positive neurons, both in glutamatergic as well as GABAergic neurons. In the adult mouse brain, however it was observed that GABAergic neurons in the hippocampus and also Purkinje cells seem to express higher levels of CDKL5 raising the possibility that the kinase plays a specific role in this neuronal subtype (Rusconi et al. 2008).

Despite a well-characterized expression pattern of the *Cdkl5* gene in time and space, very little is known about its physiological functions yet. The first hints emerged in 2005, when CDKL5 was demonstrated to possess kinase activity *in vitro* as expected based on its primary sequence (Mari et al. 2005). In fact, CDKL5 is capable of autophosphorylating both *in vitro* and *in vivo*. This activity is enhanced upon deletion of the whole C-terminal tail of the protein (from aa 298 to aa 1030); also the phosphorylation state of the TEY motif is increased in the absence of the C-terminal tail (Lin et al. 2005). All together, these results suggest an inhibitory role played by the long C-terminal tail of the protein in the modulation of its catalytic activity. The C-terminus of the protein has also been proposed to modulate the stability of the kinase; in fact, the truncated protein is expressed at higher levels than the full-length.

Recently, another possible function of the C-terminal tail was found. In cortical neurons CDKL5 is localized in both of the two main cellular compartments. Interestingly, cytoplasmic CDKL5 appears in the dendritic branches with a distinct punctuate staining. The dendritic localization of the kinase is in accordance with the overlap between CDKL5- and MAP2-positive branches in the striatum of the adult mouse brain, and raises the possibility that CDKL5 might be involved in transmitting signals form the synaptic branches to the cell nucleus or *vice versa.* The subcellular distribution between nucleus and cytoplasm was found to vary at the regional and temporal level. High CDKL5 levels in the nucleus were observed in cortex, hypothalamus and thalamus, whereas a cytoplasmic accumulation was detected in cerebellum and striatum of adult mouse brains (Rusconi et al. 2008). These data suggest that CDKL5 functions might be modulated through mechanisms regulating its subcellular localization. Interestingly, the C-terminal region of human CDKL5 has been found to be involved in regulating the subcellular distribution of the protein. In fact, full-length CDKL5 was localized both in the cytoplasm and in the nucleus of most HeLa cells expressing ectopically the protein, whereas a truncated protein devoid of the last 200 amino acids, Δ832, was almost entirely nuclear in all cells (Rusconi et al. 2008). The localization of CDKL5 in the cytoplasm is mediated by an

active nuclear export mechanism involving the nuclear export receptor CRM1 and sequences in the very C-terminal region of CDKL5. Recently, two laboratories, independently, identified a novel spice variant due to an insertion of 123 bp between exons 16 and 17 termed “exon 16a” (Rademacher et al. 2010) and “exon 16b” (Fichou et al. 2011). This exon, presently known in mouse and human, is predicted to encode an in-frame addition of 41 amino acids into the CDKL5 protein. Fichou et al. reported that in the mouse, *Cdkl5* transcripts containing this exon are expressed in all brain regions tested. Moreover, the novel exon 16a is expressed in human brain regions and human embryonic kidney 293 cells. A CDKL5 mutation search including the newly found exon 16a in a cohort of 345 female patients did not reveal any mutations in the new exon (Rademacher et al. 2010). A very recent publication described a novel splice site variant of the human and mouse CDKL5/Cdkl5 genes, which generates an alternative C-terminus. In fact, a transcript in which intron 18 is retained encodes a 107 kDa CDKL5 isoform as opposed to the conventional 115 kDa human isoform. At the molecular level, the 107 kDa isoform appears to be more stable than the longer one and be predominantly expressed in brain (Williamson et al. 2011).

So far, very few heterologous targets of the catalytic activity of CDKL5 have been identified. MeCP2 was considered an interesting candidate since the mutations in the two genes cause similar phenotypes and the activities of MeCP2 are regulated by its phosphorylation. Moreover, the temporal and spatial expression pattern of CDKL5 and MeCP2 are overlapping, suggesting that they could work in a common molecular pathway; nevertheless, there are some districts were the two genes are clearly regulated by unrelated mechanisms and CDKL5 expression is much more dynamic than that of MeCP2 (Mari et al. 2005; Rusconi et al. 2008). Importantly, CDKL5 was demonstrated to bind directly MeCP2 both *in vitro* (GST pull-down assays) and *in vivo* (co-immunoprecipitation). Moreover, the kinase was found to mediate MeCP2 phosphorylation *in vitro*, even though there are not enough data, yet, to establish whether this is exerted directly by CDKL5 or by the interposition of another co-precipitating kinase. Moreover, it still needs to be demonstrated that MeCP2 is indeed a target of CDKL5 also *in vivo*.

If the involvement of CDKL5 and MeCP2 in a common molecular pathway might help explaining the RTT-like phenotypes in patients with altered CDKL5 functions, it is likely that the distinct features characterizing these patients are caused by the

deregulation of other neuronal CDKL5 targets whose identity is still missing. Another interesting putative target of CDKL5 was aristaless (ARX) since mutations in this gene cause West syndrome that also shares common features with those caused by altered CDKL5 functions. An interesting hypothesis was that, similarly to MeCP2, CDKL5 could bind to and phosphorylate ARX. Lin and colleagues, however, were not able either to co-precipitate ARX together with CDKL5 or to appreciate any ARX phosphorylation by the kinase (Lin et al. 2005). Recently, DNA methyltransferase 1 (Dnmt1) was found to interact with CDKL5 and to be phosphorylated in vitro by a hyperactive truncated CDKL5 derivative in the presence of DNA (Kameshita et al. 2008). Recently, a novel and unexpected role of CDKL5 in the structural organization of nuclear speckles and the dynamics of their components has been described (Ricciardi et al. 2009). First of all, CDKL5 is highly enriched in the nuclear speckles, and co-localizes with SC35, a non-snRNP splicing factor of the serine-rich family of proteins, both in NIH3T3 and primary hippocampal neurons. The localization of CDKL5 is not mediated through binding to RNA, but depends on protein-protein interactions. Overexpression of CDKL5, but not the synthetic kinase-dead mutant K42R, is sufficient to induce disassembly of the speckles in both cell lines and primary human fibroblasts, indicating that the redistribution of some speckle-proteins occur in a kinase-dependent manner. Overexpression of wild-type (wt) CDKL5 affects the splicing of a reporter minigene, conversely to the kinase-dead K42R derivative. Moreover, in fibroblasts from a patient with the hypomorphic p.R175S (c.525A>T) mutation (Lin et al. 2005; Rusconi et al. 2008), SC35 puncta are lost. Down-regulation of CDKL5 by means of shRNA-mediated silencing technology leads to consistently larger speckles. Together, these results indicate that CDKL5 plays an important role in the correct maintenance of speckle structures, and for the first time, associate a function of CDKL5 with RTT. Last year, Chen and colleagues described a neuron-specific splicing variant of CDKL5 (CDKL5a) expressed markedly during post-natal development of the rat brain, and a glial isoform (CDKL5b). Down-regulation of CDKL5 in the rat brain by in utero electroporation revealed a role of the neuronal isoform of CDKL5 in regulating neuronal migration, suggesting that migratory defects might be involved in the occurrence of early seizures in patients with CDKL5 mutations. Moreover, in primary hippocampal neurons CDKL5 regulates neuronal morphogenesis through a mechanism involving Rac1 signalling (Chen et al. 2010).

## NEURONAL POLARIZATION AND shootin1

The neuron is a prime example of a highly polarized cell. The ability of cells to polarize is critical for complex biological activities, such as the organization of the nervous system. Indeed, neurons are among the best examples of a highly differentiated and polarized cell type, typically extending a long thin axon, which is engineered to propagate signals, and several shorter and thicker dendrites, which are designed to receive signal inputs. The transfer of information from a neuron to its target occurs at the synapses, which are composed of specialized pre- and post-synaptic structures. The pre-synaptic terminal stores vesicles, which upon activation, release neurotransmitters into the synaptic space, where they act on post-synaptic receptors. The asymmetric localization of proteins within the axon, dendrite, and synapse is essential for a neuron to establish its functional architecture. A lot of data has identified a number of genes products that have the capacity to impose cellular asymmetry. These proteins, that we can call polarity protein, participate in axon specification, growth, and synaptogenesis, in part through signalling to the actin and microtubule cytoskeletons.

Polarity complexes

The first complexes, the prototypic PAR (partitioning-defective) genes were originally identified in *C. elegans* for their role in directing asymmetric cell division during early development (Cowan & Hyman 2004). They encode proteins with catalytic and interaction domains characteristic of cellular signalling. PAR-1 and PAR-4 are serine/threonine kinases (Guo & Kemphues 1995; Watts et al. 2000) whereas PAR-2 is a RING finger protein (Levitan et al. 1994), PAR-5 a 14-3-3 protein that recognizes phosphorylated serine/threonine motifs (Morton et al. 2002) and both PAR-3 and PAR-6 are PDZ-domain-containing proteins (Etemad-Moghadam et al. 1995; Hung & Kemphues 1999). All these proteins can interact with one another to form larger multiprotein complexes. The other complexes are formed by interaction between PAR proteins and others. Together these polarity complexes define specific apical-basolateral domains of epithelial cells. The same mechanism could be implicated in establishing polarity and specialization in neuronal cells.

Axon Specification

The initial event in establishing a polarized neuron is the specification of a single axon. Both the establishment and maintenance of neuronal polarity involve coordinated and widespread regulation of the cytoskeleton and membrane-trafficking

machinery. The establishment of neuronal polarity has been studied extensively through the culturing of pyramidal neurons from the rodent hippocampus. The in vitro differentiation process has been divided into five stages (figure 5; Dotti et al. 1988). Shortly after plating, neurons form lamellipodia (stage one). Neurons then extend several short processes called neurites, which grow to around 20 µm before undergoing a period of extension and retraction (stage 2). Within 24 h, one of the neurites (the future axon) begins to elongate very rapidly, whereas the others (the future dendrites) undergo little extension (stage 3). After several days the remaining neurites begin to grow and acquire the characteristics of dendrites (stage 4). The axon and dendrites then reach maturation, neurons form synaptic contacts, and spontaneous electrical activity propagates throughout the neural network (stage 5). This *in vitro* system by no means recapitulates all aspects of neuronal polarization *in vivo*, where extrinsic signals from the surrounding cellular environment likely play a major role in axon and dendrite development. The neurite destined to become an axon shows particular characteristics prior to formation of the axon itself; for example, the axon-to-be develops a larger growth cone and accumulates a large number of organelles, cytosolic proteins and ribosomes (Fukata et al. 2002a; Horton & Ehlers 2003). Moreover, the motility of neurite growth cones is a consequence of high actin turnover (Bradke & Dotti 1990). Proteins associated with microtubules also influence axon specification. Therefore, the regulation of both the actin and microtubule networks appears to be a key determinant in axon development.

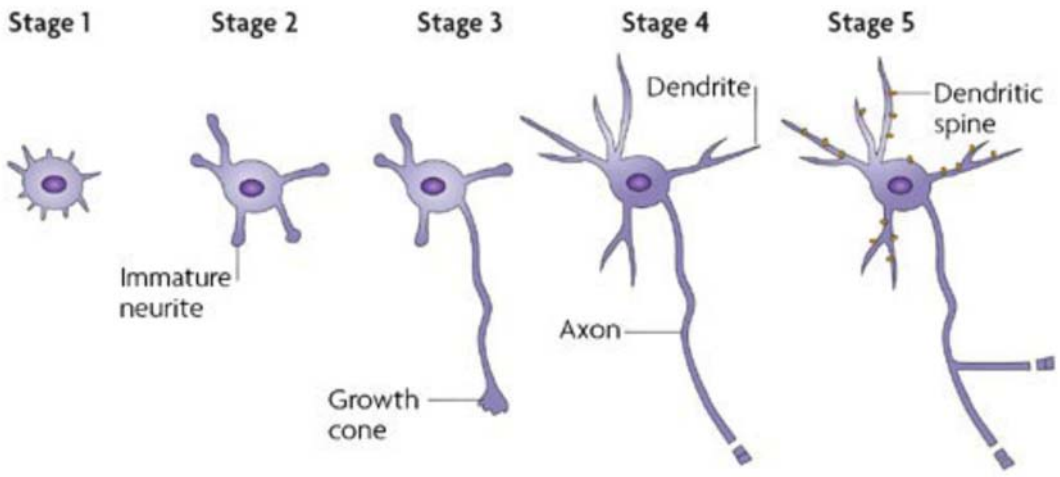


**FIGURE 5. Schematic description of stages of neuronal polarization and axon development.** Stage 1 and stage 2 occur within 24 h. Stage 3 occurs 36 h after plating; stage 4 and 5 several days after plating.

In the 2006 was identified a brain-specific protein with a spatiotemporal localization in hippocampal neurons that changed dynamically during polarization: KIAA1598, also called shootin1. It becomes upregulated, began fluctuating accumulation in multiple neurites, and eventually accumulates asymmetrically in a single neurite, which led to axon induction for polarization (Toriyama et al. 2006). Shootin1 accumulates in the growth cone stimulating neurite elongation during the transition beween stage 2 and 3 in a neurite length-dependent manner. Moreover, Toriyama et al. showed that disturbing the asymmetric organization of shootin1, such as in the overexpression experiment, induces the formation of surplus axons. Conversely, miRNA-mediated repression of shootin1 leads to significant suppression of neuronal polarization at 50 and 70 h in culture. However, at DIV7, 100% of neurons depleted for shootin1 becomes polarized suggesting that loss of shootin1 causes a delay in axonal specification.

Shootin1 is produced in the nucleus and it is actively transported to the growth cones and its retrograde diffusion to the cell body should vary inversely with neurite length. Thus, shootin1 is a good candidate molecule for the requisite positive feedback loop for axon induction (figure 6).

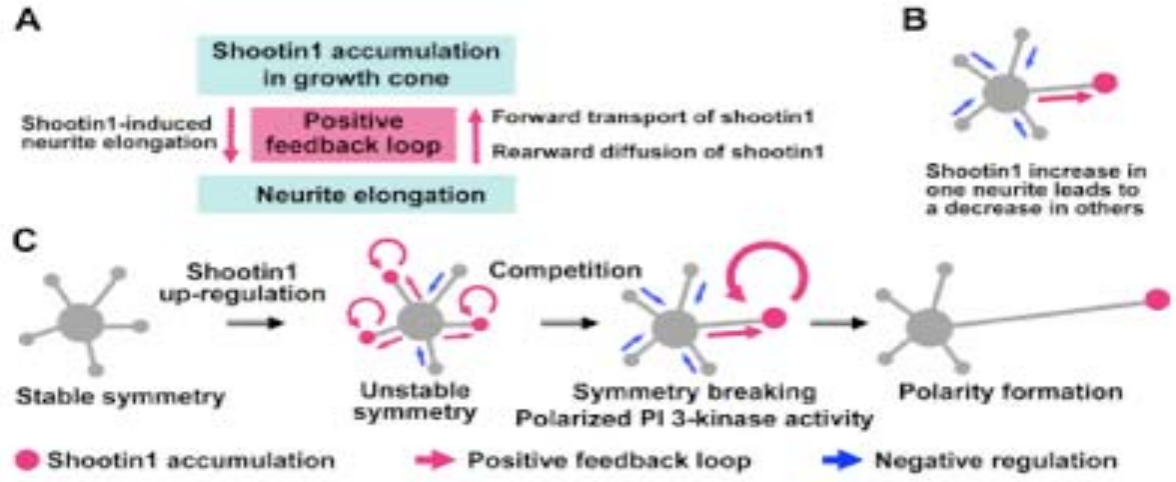


**Figure 6. Shootin1 involvement in generation of an asymmetric signal for neuronal polarization.** (A) A positive feedback loop between shootin1 accumulation in growth cone and shootin1-induced neurite elongation. (B) Competition among neurites for a limited amount of shootin1. (C) Shootin1 up-regulation triggers local positive feedback loops (red arrows) and negative regulations (blue arrows). Eventually, shootin1 will be asymmetrically accumulated in a single neurite and recruit PI 3-kinase activity there, thereby leading to neuronal polarization (Toriyama et al. 2006).

In fact, shootin1 interacts with both actin filament retrograde flow and L1-CAM in the growth cone (Shimada et al. 2008). When the actin network is disrupted by treatment with cytochalasin D, the speed of retrograde flow of shootin1 gets reduced. L1-CAM, a single-pass transmembrane protein, involved in axon outgrowth and guidance (Lemmon et al. 1989), has been show to interact with shootin1 by co-immunoprecipitation. These results suggest that shootin1 mediates the linkage between actin filament retrograde flow and L1 in growth cones. Finally, Shimada et al. detected phosphorylated forms of shootin1 in cultured hippocampal neurons. It will be intriguing to learn whether phosphorylation of shootin1 is involved in modulation of actin flow-CAM linkage, which has been implicated in regulation of axon outgrowth and guidance. Finally, it is demonstrated that shootin1 interact with PI 3-kinase, which is essential for neuronal polarization (Shi et al. 2003) and is required for spatially localized PI 3-kinase activity in hippocampal neurons, working up-stream of the kinase.

A lot of work is still to be done to enlarge our comprehension regarding the functions of CDKL5 both in physiological and in pathological contexts. For this reason, the aim of this PhD project was to identify novel interactors of CDKL5 by means of a yeast two-hybrid screen and analyze the functional role of a selected interaction partner. Given the involvement of the selected interactor for neuronal polarization and axon formation in primary hippocampal neurons, the involvement of CDKL5 in this pathway was analyzed.

# MATERIALS AND METHODS

## ANTIBODIES

The rabbit polyclonal *anti-CDKL5* antibody (Covance Research Products Inc.) was raised against CDKL5 amino acids 301-751 as described previously (Bertani et al. 2006). This antibody was used for immunoprecipitation (IP) assays. Moreover, the following antibodies were used for immunofluorescence (IF) and western blotting (WB) experiments: polyclonal *anti*-CDKL5 (WB 1:1000; IF 1:100; Sigma-Aldrich); monoclonal *anti*-actin (WB 1:5000; Sigma-Aldrich); polyclonal *anti–GAPDH* (WB 1:2000; Thermo Fisher Scientific); monoclonal *anti-β*-tubulin (Tuj1; IF 1:500; WB 1:5000; Covance); polyclonal *anti*-shootin1 (IF 1:100; WB 1:1000; Cell Signaling); monoclonal *anti*-TAU1 (IF 1:5000; CHEMICON); phalloidin-TRITC (IF 50 μg/μl; Sigma-Aldrich); *anti*-Cmyc-agarose (Sigma-Aldrich).

## PLASMIDS

Human Shootin1 Isoform 2 was amplified from ID:IOH61728 (Invitrogen) by PCR, using the following primers: 5'hshootin1 ATGAACAGCTCGGACGAAGAGAAGCAG and 3'hShooC-termISO2 CTACTGGGAGGCCAGTATTCCTTTTAGTTCTATCC and inserted into the pGEM-Teasy vector. From pGEM-Teasy-hshootin1 the sequence was amplified by PCR, using the following primers that insert a XhoI restriction site at the 5' and 3' ends and a BamHI site at the 3' end: 5'hShoot-X-B: GATCCTCGAGGATCCAACAGCTCGGACGAAG and 3'hShoot-X: GATCCTCGAGCTACTGGGAGGCCAGTATTCC. The PCR product was digested with XhoI and inserted into pECFP-C1 (Clontech) likewise digested. In parallel, the PCR product digested with BamHI and XhoI was inserted into pGEX-4T1 (Pharmacia Biotech GE Healthcare). All PCR derived constructs were sequence verified.

For shRNA experiments three short hairpin RNAs for CDKL5 (shCDKL5) were generated designing 5' phosphorylated double stranded oligos, made up of 18-nucleotide sense and antisense stems separated by a 9 amino acid loop containing a HindIII restriction site (table 2). The oligos were cloned into the pLentiLox 3.7 GFP viral vector downstream of the U6 promoter using the HpaI and XhoI restriction sites and the resulting shRNA plasmids were sequence verified. The U6 promoter driven transcripts generate stem-and-loop structures that are processed into gene-specific siRNAs targeting both human and mouse CDKL5, causing the degradation and arrest of protein expression.

| Name | Oligo Sequence |
|---|---|
| | |
| 5'hmshRNAcdkl5 | 5' P TGCTATGGAGTTGTACTTAATT**AAGCTT**ATTAAGTACAACTCCATAGCTTTTTTC 3' |
| 3'hmshRNAcdkl5 | 5' P TCGAGAAAAAAGCTATGGAGTTGTACTTAAT**AAGCTT**AATTAAGTACAACTCCATAGCA 3' |
| | |
| 5'mshcdkl5DH2 | 5' P TGGCAGCACCCAGTCTAATGTT**AAGCTT**ATATTAGACAGGGTGCTGCCTTTTTTC 3' |
| 3'mshcdkl5DH2 | 5' P TCGAGAAAAAAGGCAGCACCCTGTCTAATAT**AAGCTT**AACATTAGACTGGGTGCTGCCA 3' |
| | |
| 5'mshcdkl5Chen | 5' P TGTGAGAGCGTAAGGCCTATT**AAGCTT**AAAGGCCTTTCGCTCTCACCTTTTTTC 3' |
| 3'mshcdkl5Chen | 5' P TCGAGAAAAAAGGTGAGAGCGAAAGGCCTTT**AAGCTT**AAGAGGCCTTACGCTCTCAGGA 3' |

**TABLE 2. Primers sequences for CDKL5 shRNA** P indicate the phosphorylation at 5' end, necessary for ligation into the vector. AAGCTT is a HindIII restriction site insert for distinguish correct vector.

**YEAST TWO-HYBRID**

Yeast Two-hybrid Screen was performed from Hybrigenics Company (Hybrigenics S.A. Paris, France). The C-terminal domain of human CDKL5 (amino acids 299–1030) was cloned downstream the GAL4 DNA binding domain in the pB35 inducible vector and used as bait to screen a yeast strain co-transformed with a human adult brain cDNA library, containing, approximately 10 million independent clones. Colonies were isolated and retested for growth in minimal medium and for β-galactosidase activity.

**GST PROTEIN INDUCTION AND PURIFICATION**

Recombinant GST-shootin1 or GST alone were expressed in *E.coli* BL21 strain and induced with 0.5 mM and 0.1 mM IPTG, respectively, at 25°C with vigorous agitation for 3 hours. Following induction, the bacteria were collected by centrifugation at 6.000 *g* for 10 min and extracts were prepared by resuspending the pellet with 50 µl/ml of culture of ice-cold lysis buffer: PBS 1X (Dulbecco's phosphate buffered saline), lysozyme 100 µg/ml, 1% Triton-X100, 1 mM phenylmethylsulphonyl (PMSF; Sigma-Aldrich), 1X protease inhibitor cocktail (PIC; Sigma-Aldrich) and sonicated. Following centrifugation at 13.000 *g* for 25' at 4°C, the cleared lysate was incubated at 4°C overnight with Glutathione Sepharose 4B beads (Pharmacia Biotech, GE Healthcare) pre-equilibrated with lysis buffer. After 3 washes with lysis buffer and one with PBS 1X, proteins were eluted with 10 mM reduced glutathione. Eluted fractions containing the bulk of GST-shootin1 or GST were dialyzed against the kinase buffer (25 mM HEPES pH 7.4, 10 mM $MgCl_2$, 1 mM dithiothreitol (DTT), 0.2 mM sodium orthovanadate) and quantified by SDS-PAGE and Coomassie staining, aliquoted and stored at -80°C until phosphorylation assays.

**IMMUNOPRECIPITATION**

P7 mouse brain proteins were extracted by homogenation in lysis buffer (50 mM Tris-HCl pH 7.5, 150 mM NaCl, 1 mM EDTA, 1 mM EGTA, 1% Triton X-100, 0.1% SDS, 2 mM sodium pyrophosphate, 1 mM sodium orthovanadate), incubation on ice for 20 min and centrifugation at 100.000 *g* for 30 min at 4°C. The supernatant were incubated overnight at 4°C with 20 µl of purified *anti*-CDKL5 or 2 µl of *anti*-shootin1 or unrelated IgGs as a negative control. The immunocomplexes were precipitated with protein-G Agarose (Invitrogen). After washing with the above mentioned lysis buffer, immunocomplexes were analyzed by SDS-PAGE.

**IMMUNOFLUORESCENCE**

Hippocampal neurons were fixed in 4% para-formaldehyde and permeabilized with 5% horse serum, 0,2% Triton-X100 in TBS (Tris Buffered Saline) for 1 hour. In the same solution, the neurons were incubated overnight at 4°C with primary antibodies at the following dilutions: polyclonal *anti*-CDKL5 1:100, monoclonal *anti*-TAU1

1:5000, polyclonal *anti*-shootin1 1:100. The next day, cells were rinsed in TBS 1X three times and incubated with secondary antibodies (Alexa Flour; Invitrogen). DAPI (4',6-diamidino-2-phenylindole; IF 300 nM; Invitrogen) was used for nuclei staining. Then slices were washed and mounted in ProLong Gold antifade reagent (Invitrogen).

**IN VITRO PHOSPHORYLATION ASSAY**

For the detection of shootin1 phosphorylation, myc-tagged CDKL5 or a kinase dead derivative were immunoprecipitated from overexpressing human embryonic kidney (HEK293) cells and incubated with [γ-$^{33}$P] ATP. Briefly, cells were rinsed in cold PBS, harvested and lysed in 50 mM Tris-HCl pH 8.0, 500 mM NaCl, 0.1% Nonidet P-40, 1 mM DTT, PMSF and 1X PIC. The protein extract was pre-cleared for 1 hour with mouse IgG-agarose beads; 2 µl of purified *anti*-myc antibody was added to the cleared extract and the mixture incubated overnight at 4°C; the immunocomplexes were recovered with incubation with protein-G Agarose (Invitrogen) for 2 hours at 4°C. The complexes were washed with the above mentioned lysis buffer containing 700 mM NaCl and twice with kinase buffer (25 mM HEPES pH 7.4, 10 mM $MgCl_2$, 1 mM DTT, 0.2 mM sodium orthovanadate). After the final wash, the resin was resuspended in 20 µl kinase buffer and 1 µg of GST protein or 1.5 µg of GST-shootin1 fusion protein was added together with 50 µM ATP and 5 µCi of [γ-$^{33}$P] ATP and incubated at 30°C for 30 min. The immunocomplexes were resolved by SDS-PAGE after incubation at 70°C for 10 min, transferred to a nitrocellulose membrane that was exposed and visualized by autoradiography and quantified by PhosphorImager analysis (GE Healthcare). The presence of protein was verified by western blottling using *anti*-CDKL5 and *anti*-shootin1 antibodies.

**TWO-DIMENSIONAL ISOELECTRIC FOCUSING**

Cells were collected in PBS 1X, after centrifugation at 1000 *g* for 5 min pellet was resuspended in UTC buffer (7 M urea, 2 M thiourea, 4% CHAPS) and quantificated by Bradford method. Two-dimensional isolectric focusing (IEF) was performed according to Görg (Görg et al. 2000), with minor modifications. Samples (about 200 ug) were diluted to 125 ul with a buffer containing 7 M urea, 2 M thiourea, 4%

CHAPS, 1% IPG buffer 4-7, 50 mM DTT and traces of bromophenol blue, and loaded on 7 cm IPG DryStrips with a linear 4-7 pH gradient by in-gel rehydration (1 h at 0 V, 10 h at 50 V). IEF was performed at 20°C on IPGphor II (GE Healthcare) according to the following schedule: 2 h at 200 V, 2 h linear gradient to 2000 V, 2 h at 2000 V, 1 h of linear gradient to 5000 V, 2 h at 5000 V, 2 h linear gradient to 8000 V and 2 h and 30 min at 8000 V. IPG strips were then equilibrated for 2 × 30 min in 50 mM Tris-HCl pH 8.8, 6 M urea, 30% glycerol, 2% SDS and traces of bromophenol blue containing 1% DTT for the first equilibration step and 2.5% iodoacetamide for the second one. SDS-PAGE was performed using 8% 1.5 mm thick separating polyacrylamide gels without stacking gel, using Biorad system (Biorad). Molecular weight marker proteins (11-250 kDa, Euroclone) were used for calibration. Proteins were detected with *anti*-shootin1 and *anti*-Tuj1 antibodies.

**SUBCELLULAR FRACTIONATION**

Total brain lysate was fractionated by differential centrifugation. Briefly, the brain tissue was homogenated in lysis buffer (50 mM Tris-HCl pH7.5, 150 mM NaCl, 1 mM EDTA, 1 mM PMSF, 1 mM sodium orthovanadate, 1X PIC) and the nuclear fraction was separated by centrifugation at 1500 *g* for 15 min at 4°C. The pellet was resuspended directly in sample buffer and stored until use. The supernatant (PNS post-nuclear supernatant) was centrifugated at 13.000 *g* for 25 min at 4°C to separate the mitochondrial fraction (pellet). The second supernatant was centrifugated at 100.000 *g* for 45 min at 4°C to separate cytosol (supernatant) and the rest of the membrane (pellet).

**CELL CULTURES AND TRANSFECTIONS**

HEK293 cells were maintained in Dulbecco's modified Eagle's medium (D-MEM) supplemented with 10% fetal bovine serum, 2 mM L-Glutamine and 100 U/mM Penicillin-Streptomycin and grown at 37°C with 5% $CO_2$. Transient transfections were performed with the calcium phosphate method using 40 µg of DNA for 15 cm diameter dishes where around 1 million of cells were plated the day before.

Cortical or hippocampal neurons were prepared from the brain of mouse embryos at embryonic day (E) 17 or 18. Hippocampi and cortices were removed from brains and

put into the HBSS (Hanks'Balanced Salt Solution 1X, Invitrogen) prewarmed at 37°C. After collecting all tissues, HBSS were removed by decanting and replaced with prewarmed trypsin-EDTA and incubated at 37°C for 10 min. After trypsinization, and washing in HBSS, hippocampi and cortices were triturated by gently pipetting up and down with a fire-polished Pasteur pipette until all tissue was dissociated.

After counting, 20.000 hippocampal neurons were plated on 1 mg/ml poly-L-lysine (Sigma-Aldrich) treated coverslips for immunofluorescence and grown in N-MEM with B27 supplement, prewarmed and equilibrated to pH 7.4 at 37°C and 5% $CO_2$, and 100.000 hippocampal neurons were plated on 0.1 mg/ml of poly-L-lysine for western blot experiments. ARA-C (2.5 μM) was added after four days in culture.

**VIRUS PREPARATION AND INFECTION**

Viral supernatant was prepared in HEK 293T cells transfecting with the four vectors listed below using the calcium phosphate method:

- pMDL
- pREV
- pVSVG
- pLL3.7-shRNA.

After overnight incubation at 37°C, 5% $CO_2$, the medium was changed and 30 hours later the medium was collected and filtrated (0.22 μm filter). By centrifugation at 20.000 *g* for 2 h at 20°C, viral particles were pelleted and resuspended in 80 μl of PBS 1X by gently agitation overnight at 4°C and stored at -80°C until use.

Primary neurons were infected by the ratio 1 μl:200.000 cells. Viral particles were resuspended well by pipeting in a small amount of neuronal medium and added the neuronal cultures at the same time of plating.

**CELLS MEDIUM AND SOLUTION**

**D-MEM**: D-MEM 1X (Invitrogen)
Fetal bovin serum (FBS) 10% (Euroclone)
L-glutamine 200 mM (Euroclone)
Penicilline/Streptomicine 1X (Euroclone)

**N-MEM:** MEM 10X (Invitrogen)
B-27 2% (Invitrogen)
Sodium piruvate (Gibco)
L-glutamine 200 mM (Euroclone)
Sodium bicarbonato 26 mM
D-Glucose 33 mM

**D-MEM-HS:** D-MEM+GlutaMax (Invitrogen)
Hourse serum (HS) 10%
L-glutamine 200 mM (Euroclone)
Sodium piruvate (Gibco)

**TRYPSIN-EDTA** (Gibco)

**HBSS** (Gibco)

# RESULTS

## ANALYSIS OF THE YEAST TWO-HYBRID ASSAY RESULTS

As discussed previously, mutations in *CDKL5* cause several forms of mental retardation, including the Hanefeld variant of RS. This variant is characterized by a subset of symptoms that differ from those normally found in patients with the classic form, indicating that this pathology could be due to the disruption of some molecular pathways different from those altered by a malfunctioning MeCP2. In order to understand the role of CDKL5 in Rett syndrome and in the central nervous system, we decided to perform a yeast two-hybrid screening to provide a number of candidate genes that could be interactors of CDKL5 and thereby indicate the molecular pathway(s) associated to *CDKL5*.

The screening was performed by an external service, Hybrigenics, which is highly specialized in performing high throughput yeast two hybrid screens. Besides providing a highly qualified technical service, Hybrigenics also delivers the final list of interactors with a biological confidence score, which helps identifying the true positive interactors. As bait, we decided to use the unique C-terminus of CDKL5, comprised between amino acids 299 and 1030, that regulates various aspects of the activities of this kinase, including the catalytic activity, subcellular localization, and protein stability (Bertani et al. 2006, Rusconi et al. 2008; Williamson et al. 2011). In the initial tests, this bait was found not to auto-activate the yeast gene reporters but to be highly toxic. Therefore, the company decided to use an inducible vector to express the $GAL4_{DBD}$-CDKL5 fusion protein constituting the bait. This second strategy was useful to bypass the toxicity and a human adult brain cDNA library, containing approximately 10 million independent clones, was screened. By testing more than

100 million clones, the complexity of the library was covered more than 10 times and 170 positive clones were isolated. The complete list of CDKL5 interacting proteins is shown in table 2. We analysed the nature of the identified interactors and the first indication was that CDKL5 might be involved in four specific pathways. In the following list the capital letter after the name of the single gene indicates the biological confidence score: **A** very high confidence; **B** high confidence; **C** good confidence; **D** moderate confidence.

*FIRST: NEURONAL POLARIZATION*

- *KIAA1598*: (**A**) this gene encodes shootin1, a protein essential for axonal elongation and neuronal polarization (Toriyama et al. 2006);
- *FMNL2*: (**B**) encodes formin-like 2. Formin-related proteins have been implicated in morphogenesis, cytokinesis, and cell polarity. Interestingly, a microdeletion including *FMNL2* is associated with mental retardation (Lybaek et al. 2009);
- *GPRASP2*: (**B**) the protein encoded by this gene is member of a family that regulates the activity of G protein-coupled receptor (GPCRs). The encoded protein has been shown to be capable of interacting with several GPCRs, including the M1 muscarinic acetylcholine receptor and the calcitonin receptor (Horn et al. 2006);
- *GRLF1*: (**B**) this gene encodes for glucocorticoid receptor DNA binding factor 1, also called p190A, one of the two p190 RhoGAP proteins that constitute the major inhibitors of Rho GTPase activity in mammalian cells. Mice devoid of p190A show several defects in neuronal development indicating a role of the protein in axonal outgrowth and/or guidance (Tomar et al. 2009; Matheson et al. 2006). Regarding this putative interaction, it is worthwhile to note that recently Chen et al. (2010) demonstrated that CDKL5 is involved in BDNF-Rac1 signaling, forming a complex with Rac1, a very important Rho GTPase important regulators of neuronal development and function (Reichardt 2006).

*SECOND: CYTOSKELETON*

- *DSP:* (**D**) codes for desmoplakin, an obligate component of functional desmosomes that anchors intermediate filaments to desmosomal plaques. Mutations in this gene are the cause of several cardiomyopathies and keratodermas (Uzumcu et al. 2006);

- *DST*: (**D**) this gene encodes dystonin a member of the plakin protein family of adhesion junction plaque proteins. It has been shown that some isoforms are expressed in neuronal and muscle tissues, anchoring neural intermediate filaments to the actin cytoskeleton. Consistent with the expression profile, mice defective for dystonin show skin blistering and neurodegeneration (Young et al. 2008);
- *SPTBN1*: (**E**) spectrin, beta, non-erythrocytic 1. Spectrin is an actin cross-linking and molecular scaffold protein that links the plasma membrane to the actin cytoskeleton and functions in the determination of cell shape, arrangement of transmembrane proteins, and organization of organelles (Hu et al. 1992).

*THIRD: TRANSPORT AND AXONAL TRANSPORT*

- *KIF5A*: (**D**) this gene encodes a member of the kinesin family of proteins, which is part of a multisubunit complex that functions as a microtubule motor in intracellular organelle transport. Mutations in this gene cause autosomal dominant spastic paraplegia 10 (Tessa et al. 2008);
- *NEFL*: (**D**) this gene encodes the light chain neurofilament protein (68kDa). Neurofilaments comprise the axoskeleton and they functionally maintain the neuronal calibre. They may also play a role in intracellular transport to axon and dendrites. Mutations in this gene cause Charcot-Marie Tooth disease (Reilly et al. 2009).

*FOURTH: CELL SIGNALLING AND DEGRADATION*

- *SPRY2*: (**B**) encodes a protein belonging to the Sprouty family of proteins, which are evolutionarily conserved inhibitors of tyrosine kinase signaling. In the primary dermal endothelial cells this gene is transiently upregulated in response to fibroblast growth factor two. Interestingly this protein may play a role in alveoli branching during lung development as shown by a similar protein (Yusoff et al. 2002);
- *SPRED2*: (**C**) is a member of the Sprouty/SPRED family of proteins that regulate growth factor-induced activation of the MAP kinase cascade (Nonami et al. 2004);
- *ASB3*: (**D**) encodes a member of the ankyrin repeat and SOCS box-containing family of proteins. This protein is believed to be involved in substrate

recognition of proteins destined to ubiquitination and subsequent proteasomal degradation (Chung et al. 2005);

- *KLHL7*: (**D**) encodes a BTB-Kelch-related protein. The encoded protein may be involved in protein degradation;
- UBE4A: (**B**) encodes the ubiquitination factor E4A. The modification of proteins with ubiquitin is an important cellular mechanism for targeting abnormal or short-lived proteins for degradation (Contino et al. 2004; Sakiyama et al. 2008).

Altogether, the nature of the identified interactors places CDKL5 in different molecular networks involved in regulating distinct aspects of neuronal functions. As indicated, the various interactions have been assigned different degrees of confidence with only shootin1 has obtained the highest confidence score. We thus decided to analyze in more details the interaction between shootin1 and CDKL5 and to investigate the putative role of CDKL5 for neuronal polarization.

**CDKL5 INTERACTS WITH SHOOTIN1 *IN VIVO* BUT NOT *IN VITRO***

In 2006 Toriyama et al. analyzing the expression levels of shootin1 in different adult rat tissues described it as a brain specific protein. Furthermore, the authors analysed the temporal expression pattern of shootin1 during the pre- and post-natal stage, indicating that in rat brain shootin1 is relatively low at embryonic life 15 (E15), peaks around P4, and decreases at P14. In the adult brain the protein is under detection limit, suggesting that its expression is limited to the early brain developmental stages. Considering the fact that shootin1 levels decrease towards the end of neuronal maturation, whereas CDKL5 remains at high levels up to the adulthood (Rusconi et al. 2008). In this context, we decided to compare the expression patterns of the two proteins starting from E18, throughout different stages of mouse development until adulthood (P120). Total brain extracts obtained from different aged mice were analysed by western blotting analysis. According to previous results published by our laboratory in 2008, and reconfirmed from Chen et al. in 2010, we observed a robust up-regulation of the kinase in the perinatal period: in fact, the protein was almost undetectable, at E18 and P1 and its expression gradually increased in the early post-natal stages. CDKL5 levels stabilized around P14 and persisted during adulthood (figure 7A). In accordance with the published results, shootin1 expression levels

increased from E18, where it is evidently present, to P4 and slowly declined up to the adult, where the levels are under detection limit (figure 7A, upper panel). The observations were confirmed by quantifications performed by normalizing the specific CDKL5 or shootin1 signal to that of Tuj1 (figure 7A, lower panel). The expression profiles of the two proteins could be consistent with the hypothesis that they work in a common molecular pathway during P4/P7 post-natal stages.

In the past years, several authors (Bertani et al. 2005; Lin et al. 2005; Rosas Vargas et al. 2008; Rusconi et al. 2008) characterized the expression pattern of CDKL5 in transfected cells and tissues showing both nuclear and cytoplasmic localization. Shootin1 is accurately described as a cytosolic protein soluble with low detergent concentration (Toriyama et al. 2006) and Shimada et al. (2008) published that shootin1 interacts with actin filament retrograde flow and L1-CAM in growth cones, where it accumulates. Having demonstrated that shootin1 and CDKL5 might work together in a specific temporal stage (P4/P7), we analysed the abundance of the two proteins in a cytosolic soluble fraction devoid of membranes, at different developmental stages. As we can observe in figure 7B, in the soluble cytosolic fraction CDKL5 levels remain relatively high up to P7, after which stage they drastically reduce. Shootin1 levels remain almost constant throughout all the analysis. By comparing the signals obtained in panels A and B, it appears evident how this fractionation protocol permits to enrich in shootin1, therefore making it detectable even in the adult samples. We proceeded investigating the interacion between the two proteins by co-immunoprecipitation using the soluble cytosolic fraction obtained from P7 mouse brain. When shootin1 was specifically immunoprecipitated, CDKL5 could be detected in the pellet, whereas it could not be revealed when unrelated IgGs were used as negative control (figure 8A). In the reciprocal experiment, shootin1 could also be specifically co-immunoprecipitated with CDKL5 (figure 8B). The bands appearing under shootin1 represent the light chains of the immunoglobulin. It is worthwhile to note that co-expressing exogenous shootin1 and CDKL5 in HEK293 cells, we are not able to detect any co-immunoprecipitation between the two proteins (data not shown). Altogether our results demonstrate that shootin1 and CDKL5 associate in a common complex *in vivo* at least in the nervous system.

## CDKL5 IS REGULATED DURING NEURONAL POLARIZATION AND CO-LOCALIZES WITH SHOOTIN1 IN THE AXONAL GROWTH CONE

Shootin1 was published to be a brain specific protein, with a key role in neuronal polarization (Toriyama et al. 2006), a very rapid and specific mechanism that occurs few hours after plating, as described in the introduction. Considering the molecular interaction between CDKL5 and shootin1, we decided to investigate the involvement of CDKL5 in the same pathway. At first, we studied the expression pattern of CDKL5 during polarization stages. It has been published that in cultured rat hippocampal neurons shootin1 levels increase remarkably during stages 2/3 of neuronal polarization and remain high up to DIV14; thereafter levels progressively decrease up to DIV28, when neuronal maturation is complete (Toriyama et al. 2006). Using the widely accepted model system based on mouse hippocampal neurons, we analysed the expression levels of CDKL5 and compared it with those of shootin1. Total neuronal extracts were collected at 24, 40, 72, 96 h, and DIV7, and visualized by western blotting analysis. According to the published data, we observed that endogenous shootin1 is upregulated during neuronal maturation in mouse neurons up to DIV7, whereas it decreases in mature neurons (DIV28; figure 9). Concerning CDKL5, the analysis indicate that it is undetectable at 24 h, and weakly expressed at 40 h after plating, but when maturation proceeds it becomes more and more expressed reaching a peak at 96 h. The concurrent presence of the two proteins up to DIV7, and the well-known role of shootin1 in the cone growth, open the possibility that the observed molecular interaction could be important during the first stages of neuronal maturation. Thus, we decided to examine the localization of endogenous CDKL5 in developing neurons with a special interest in the growth cone. Hippocampal neurons were fixed at 24 h and 48 h after plating and immunostained for CDKL5 (figure 10A; red); nuclei were visualized by DAPI staining (blue). In young neurons fixed at 24 h, when the extensions are still undistinguishable neurites, CDKL5 appears well distributed all over the cell, with a clear accumulation at the tip of the neurites (arrowheads). When the axon is already chosen (stage IV), a good fraction of CDKL5 appeared to be accumulated in the growth cone of the longer process, that is likely to become the axon (48 h; figure 10A). On the contrary, when neurons were mature, CDKL5 seemed to be restricted in the cell soma with a diffuse staining and without any signs of accumulation in the distal tips (data not shown).

We proceeded investigating the co-localization of CDKL5 and shootin1 in the growth cones. As shown in figure 10B, CDKL5 and shootin1 co-localized in hippocampal neurons fixed at 18 h and 36 h after plating. In particular, we noticed evident staining in the axonal growth cone, where CDKL5 and shootin1 appeared co-localized (figure 10C arrowheads and enlargement), but not along the neurite (figure 10C white arrows). Altogether, these results prompted us to investigate whether CDKL5 participates in the early stages of neuronal polarization, possibly in combination with shootin1. Furthermore, the presence of CDKL5 in the growth cones opens the possibility of a new cytoplasmic role of the kinase.

**EVALUATION OF shRNA PLASMIDS FOR CDKL5**

In order to definitely prove the involvement of CDKL5 in neuronal polarization, we cloned in a suitable GFP expressing lentiviral vector (pLentiLox 3.7 GFP), three oligonucleotides that, once transcribed form the so-called short hairpin RNAs (shRNA) that get processed within the cells to small interfering RNAs that bind to the complementary mRNA of CDKL5 promoting its ablation. We verified the efficiency of our constructs by lentiviral infection of hippocampal and cortical primary neurons. Neurons from E17 mice were infected at the time of plating and cultured for 48 and 72 h or up to DIV 7 (figure 11). Total extracts were collected and the expression levels of CDKL5 were visualized by western blotting analysis: the expression of the kinase in control infected neurons was considered as basal level of CDKL5 in neurons (lanes 1, 2, 6, 7, 11, 12). Considering this control, CDKL5 is reduced in the cells infected with shCDKL5DH1 starting from 72 h, and drastically reduced at DIV7 after infection. shCDKL5DH2 has a minor effect (lanes 4, 9, 14) whereas in our hand the published shRNA shCDKL5Chen (Chen et al. 2010; lanes 5, 10, 15) has no effect. Therefore, considering the obtained results, next loss-of-function experiments have been performed with shLacZ and shCDKL5DH1.

**CDKL5 REGULATES NEURONAL POLARIZATION OF CULTURED HIPPOCAMPAL NEURONS THROUGH shootin1.**

To determine the effect of CDKL5 knock-down on neuronal development, we infected cultured hippocampal neurons at the time of plating with shLacZ and shCDKL5DH1, and analyzed neuronal development. Notably, the ablation of CDKL5 has a dramatic effect on neuronal network formation (figure 12A), in fact, the interfered neurons

show less processes extending from the cell bodies (figure 12A enlargement), as already published by Chen et al. (2010). We proceeded analyzing if this effect might be due to a defect in neuronal polarization (Dotti et al. 1987; Goslim et al. 2001). When hippocampal neurons form a single axon, identified by Tau-1 staining with a proximal to distal increase in intensity, and several minor neurites, they are classified as normally polarized. If the normal polarization is disturbed, neurons are indicated as unpolarized: they can form two or more axons (hyperpolarized) or fail to specify a neurite to become an axon (hypopolarized; figure 12B). In loss-of-function experiments, the establishment of neuronal polarity was analyzed 48, 72, 96 h and DIV7 after plating, and the statistical analysis was done counting polarized and unpolarized neurons (figure 12C). Infected cells are distinguished through their GFP signal. At 48 h the majority (means $\pm$ SEM: 62,8% $\pm$ 6,1%; n= 128) of control neurons show a normal polarization with one neurite positive for Tau-1. In contrast to that, the suppression of CDKL5 decreases the polarized phenotype up to 32% $\pm$ 3,7% of the cells (n = 109; $p< 0.01$). At 72 h the percentage of polarized control neurons increases (means $\pm$ SEM: 72,5% $\pm$ 3,9%; n= 120), whereas in interfered neurons the number decreases (means $\pm$ SEM: 29% $\pm$ 3,9%; n= 133). At 96 h we observed a further increase of polarized neurons in control samples (means $\pm$ SEM: 80% $\pm$ 4,3%; n= 137) as well as in the knock-down sample (means $\pm$ SEM: 49% $\pm$ 0,2%; n= 144; figure 12C). At DIV7 the mean of polarized neurons remains around 50%, considering polarized the cells showing one Tau-1 positive neurite, but their morphology appears disorganized, very different from typical polarized shape. This result suggests that a deficiency of CDKL5 causes a defect in neuronal polarization that persists till the end of stage IV where the neurites have normally differentiated into axon and dendrites. In addition, to demonstrate that it is not an off-target effect, we performed the same analysis with the shCDKL5DH2 plasmid and we obtained a similar result, but with a milder effect, in accordance with its minor knock-down efficiency (data not shown). To directly test whether CDKL5 might be involved in neuronal polarization through shootin1, we analyzed shootin1 localization in hippocampal neurons, expressing shLacZ and shCDKL5DH1, at 72 h. At this time, shootin1 is still accumulated in the axon and silencing of CDKL5 has already started. Shootin1 localization in control neurons appears normal (shLacZ figure 13A), whereas in knock-down neurons it disappears along the axon and remains localized in the soma (shCDKL5DH1 figure 13A). To analyze if the absence of shootin1 in the

axon, is due to a delocalization or a reduction of the protein levels, we quantified the total signal of shootin1, in control and interfered cells. As show in figure 13B the quantity of shootin1 remains invariable (mean ± SEM 10.77 ± 0.58 shLacZ; 10.76 ± 0.50 shCDKL5DH1). Taken together, these results indicate that CDKL5 may affect neuronal polarization in a shootin1-dependent manner. Since CDKL5 is a protein kinase, and Shimada et al. published in 2008 that shootin1 exists in different phosphorylated forms, we investigated if shootin1 is a substrate of CDKL5. Total extracts were collected at DIV7 after shRNA mediated silencing, and the electrophoretic pattern of shootin1 analyzed by two-dimensional isoelectric focusing. As shown in figure 14A and B, in the control, shootin1 appears in five isoforms with a pI between pH 5 and 6 (shLacZ); when CDKL5 is suppressed the number of isoforms appears almost equivalent but there is a clear shift towards a more basic pH. This result is consistent with the loss of phosphate ($PO_4^{3-}$) group(s) but more experiments, including phosphatase treatment, are required to unequivocally determine if shootin1 is a CDKL5 substrate.

**CDKL5 ABLATION AFFECTS NEURONAL MORPHOGENESIS**

Based on the above results, it seems that the interaction between CDKL5 and shootin1 affects neuronal polarization. However, our results and those recently published by Chen et al. (2010), show that CDKL5 affects neuronal phenotype in multiple manners. Chen et al. published that CDKL5 regulates neuronal morphogenesis through the Rho-GTPase Rac1, a well known regulator of actin dynamics and neuronal morphogenesis. We observed that, even if a significant quantity of neurons has a Tau-1-positive neurite at 96 h and at DIV7 (around 49%; figure 15), therefore corresponding to polarized cells, the morphology of the same cells does not show the typical asymmetry, but rather a disorganized and almost symmetrical structure. Indeed, as shown in figure 15A (lower panel), the majority of neurons has a lot of processes emerging from the cell body that have, apparently, the same length. This phenotype persists up to DIV7 (figure 15B); at this stage the processes have become longer but often remain indistinct (figure 15B arrowheads) or disorganized (figure 15B arrows). This result indicates that, there might be adestruction/disorganization of the scaffold of the cell.

| Clone Name | Type Seq | Gene Name (Best Macth) | Start...Stop (nt) | Frame | Sens | % Id 5p | % Id 3p | PBS |
|---|---|---|---|---|---|---|---|---|
| pB35_B-190 | 3p | Homo sapiens - KIAA1598 | ..880 | ?? | | | 83.2 | A |
| pB35_B-136 | 5p/3p | Homo sapiens - KIAA1598 | 27..1062 | IF | | 99.4 | 98.6 | A |
| pB35_B-27 | 5p/3p | Homo sapiens - KIAA1598 | 93..876 | IF | | 99.9 | 97 | A |
| pB35_B-176 | 5p/3p | Homo sapiens - KIAA1598 | 93..876 | IF | | 100 | 99 | A |
| pB35_B-159 | 5p/3p | Homo sapiens - KIAA1598 | 114..870 | IF | | 99.6 | 97.7 | A |
| pB35_B-43 | 5p/3p | Homo sapiens - KIAA1598 | 114..870 | IF | | 99.7 | 99.1 | A |
| pB35_B-178 | 5p/3p | Homo sapiens - KIAA1598 | 159..880 | IF | | 99.9 | 98.9 | A |
| pB35_B-105 | 5p/3p | Homo sapiens - FMNL2 | 156...1443 | IF | | 99.4 | 99.1 | B |
| pB35_B-132 | 5p/3p | Homo sapiens - FMNL2 | 669...1382 | IF | | 99.9 | 97.9 | B |
| pB35_B-187 | 5p | Homo sapiens - FMNL2 | 680 | IF | | 99.7 | | B |
| pB35_B-104 | 5p/3p | Homo sapiens - GPRASP2 | 1551..2475 | IF | | 99.9 | 99.7 | B |
| pB35_B-31 | 5p/3p | Homo sapiens - GPRASP2 | 1575..2448 | IF | | 99.9 | 97.9 | B |
| pB35_B-164 | 5p/3p | Homo sapiens - GPRASP2 | 1722..2448 | IF | | 97.1 | 97.6 | B |
| pB35_B-121 | 5p | Homo sapiens - GPRASP2 | 1728 | IF | | 98.5 | | B |
| pB35_B-58 | 5p/3p | Homo sapiens - GRLF1 | 1107..2231 | IF | | 99.9 | 98.9 | B |
| pB35_B-110 | 5p/3p | Homo sapiens - GRLF1 | 1107..2231 | IF | | 99.9 | 98.4 | B |
| pB35_B-70 | 5p/3p | Homo sapiens - GRLF1 | 1218..2230 | IF | | 99.9 | 99.5 | B |
| pB35_B-53 | 5p/3p | Homo sapiens - GRLF1 | 1218..2230 | IF | | 99.9 | 98.5 | B |
| pB35_B-87 | 5p | Homo sapiens - GRLF1 | 1434 | IF | | 99.8 | | B |
| pB35_B-140 | 5p/3p | Homo sapiens - DSP | 1572..2343 | IF | | 99.9 | 97.3 | D |
| pB35_B-41 | 5p/3p | Homo sapiens - DST | 13476..14760 | IF | | 99.6 | 96.4 | D |
| pB35_B-169 | 5p/3p | Homo sapiens - SPTBN1 | 4605..5481 | IF | | 99.9 | 97.8 | E |
| pB35_B-69 | 5p/3p | Homo sapiens - KIF5A | 1260..2055 | IF | | 99.3 | 97.3 | D |
| pB35_B-50 | 5p/3p | Homo sapiens - KIF5A | 1260..2055 | IF | | 99.4 | 98.3 | D |
| pB35_B-160 | 5p/3p | Homo sapiens - NEFL | 399..1200 | IF | | 99.3 | 97.5 | D |
| pB35_B-49 | 5p/3p | Homo sapiens - NEFL | 399..1200 | IF | | 99.7 | 99.5 | D |
| pB35_B-99 | 5p/3p | Homo sapiens - SPRY2 | 213..814 | IF | | 100 | 99.3 | B |
| pB35_B-120 | 5p/3p | Homo sapiens - SPRY2 | 303..841 | IF | | 100 | 99.8 | B |
| pB35_B-44 | 5p/3p | Homo sapiens - SPRY2 | 303..841 | IF | | 99.8 | 100 | B |
| pB35_B-122 | 5p/3p | Homo sapiens - SPRED2 | 648..1284 | IF | | 99.7 | 97.4 | C |
| pB35_B-108 | 5p/3p | Homo sapiens - SPRED2 | 927..1391 | IF | | 99.8 | 99.8 | C |
| pB35_B-151 | 5p/3p | Homo sapiens - ASB3 | -133..922 | IF | | 99.7 | 98.7 | D |
| pB35_B-72 | 5p/3p | Homo sapiens - KLHL7 | 189..824 | IF | | 97.8 | 98.4 | D |
| pB35_B-60 | 5p/3p | Homo sapiens - KLHL7 | 189..824 | | | 99.8 | 99.1 | D |
| pB35_B-95 | 3p | Homo sapiens - UBE4A | ..834 | ?? | | | 91.1 | B |
| pB35_B-39 | 5p/3p | Homo sapiens - UBE4A | 147..1082 | IF | | 99.2 | 96.5 | B |
| pB35_B-96 | 5p | Homo sapiens - UBE4A | 147 | IF | | 97.1 | | B |
| pB35_B-181 | 5p | Homo sapiens - UBE4A | 147 | IF | | 100 | | B |
| pB35_B-5 | 5p/3p | Homo sapiens - UBE4A | 147..1082 | IF | | 99.9 | 98.9 | B |
| pB35_B-63 | 5p/3p | Homo sapiens - UBE4A | 147..1082 | IF | | 99.7 | 98.7 | B |
| pB35_B-128 | 5p/3p | Homo sapiens - UBE4A | 147..1082 | IF | | 98.9 | 98.9 | B |
| pB35_B-71 | 5p/3p | Homo sapiens - UBE4A | 192..834 | IF | | 100 | 98.6 | B |
| pB35_B-83 | 5p/3p | Homo sapiens - UBE4A | 192..834 | IF | | 99.8 | 99.8 | B |

**TABLE 2: Parameter of confidence of the main interactors.** Start..Stop (nt): position of the 5p and 3p prey fragment ends, relative to the position of the ATG start codon (A=0); Frame, with regard to the theoretical frame of each corresponding CDS (GeneBank), fragments are cloned in frame (IF) if they are in frame with Gal4AD or an unidentified frame (??) when the clone sequence is antisense or when the 5p sequence is missing. PBS: score that is automatically computed through algorithms;A: very high confidence in the interaction; B: high confidence; C: good confidence; D: moderate confidence, contains false positives and hardly detectable interactions; E: likely to be non-specific interactions; F: experimentally proven

artifacts.

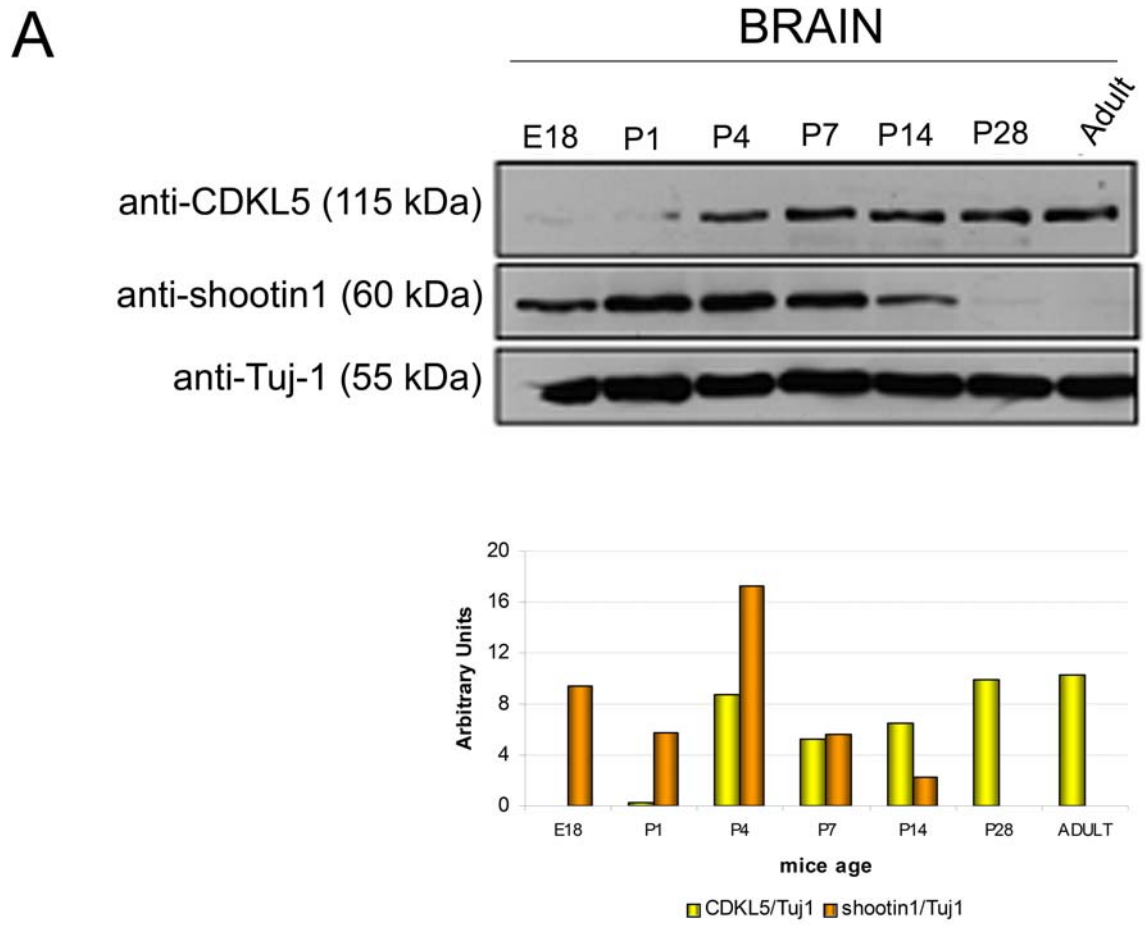


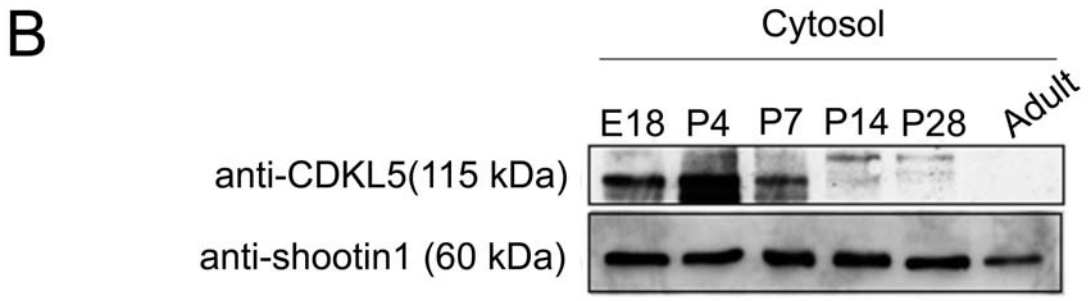


**FIGURE 7. CDKL5 expression compared with shootin1. A.** Western blotting showing CDKL5 and shootin1 protein levels in total brain lysates at E18, P1, P4, P7, P14, P28 and adult stages (upper panel). Tuj1 was used as a loading control. CDKL5 and shootin1 protein levels were quantified and normalized to Tuj1 (lower panel). **B.** Western blotting showing CDKL5 and shootin1 levels in the soluble cytosolic fractions obtained from mouse brains at E18, P4, P7, P14, P28 and adult stages. Cytosol: supernatant after centrifugation at 100.000 *g*.

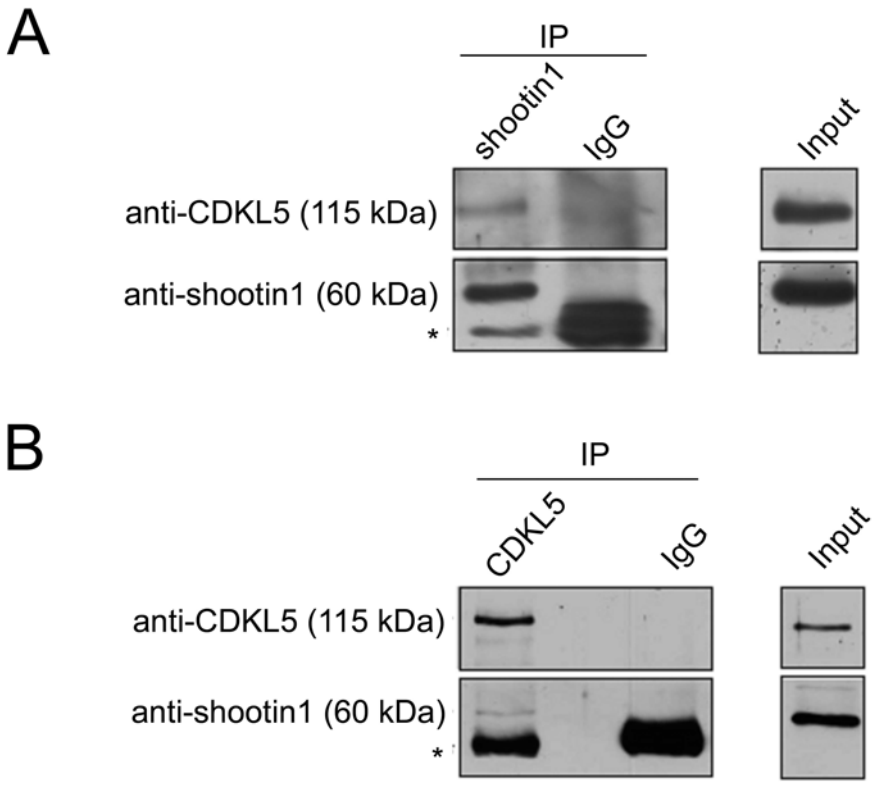


**FIGURE 8. CDKL5 associates with shootin1.** Co-immunoprecipitation of shootin1 **(A)** and CDKL5 **(B)** from P7 mouse brain lysates. Brain lysates were incubated with antibodies against shootin1, CDKL5 or, as control, with IgG. The immunoprecipitates were analysed by immunoblotting with anti-shootin1 and anti-CDKL5 antibodies. Input: brain lysate; * heavy chain immunoglobulin.

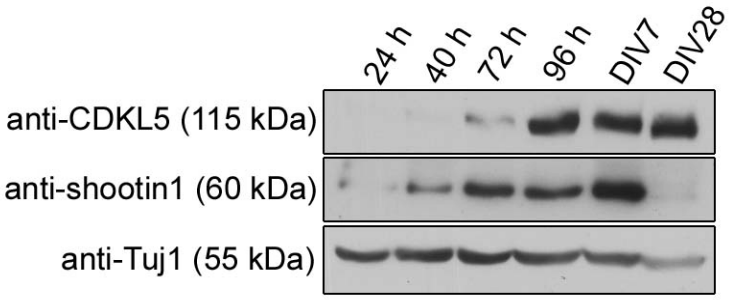


**FIGURE 9. CDKL5 and shootin1 levels are regulated during neuronal maturation.** Primary hippocampal neurons prepared from E18 mouse embryos were lysed at the indicated time points and the levels of CDKL5 and shootin1 analyzed by WB using Tuj1 as loading control. DIV= days in vitro; h= hours.

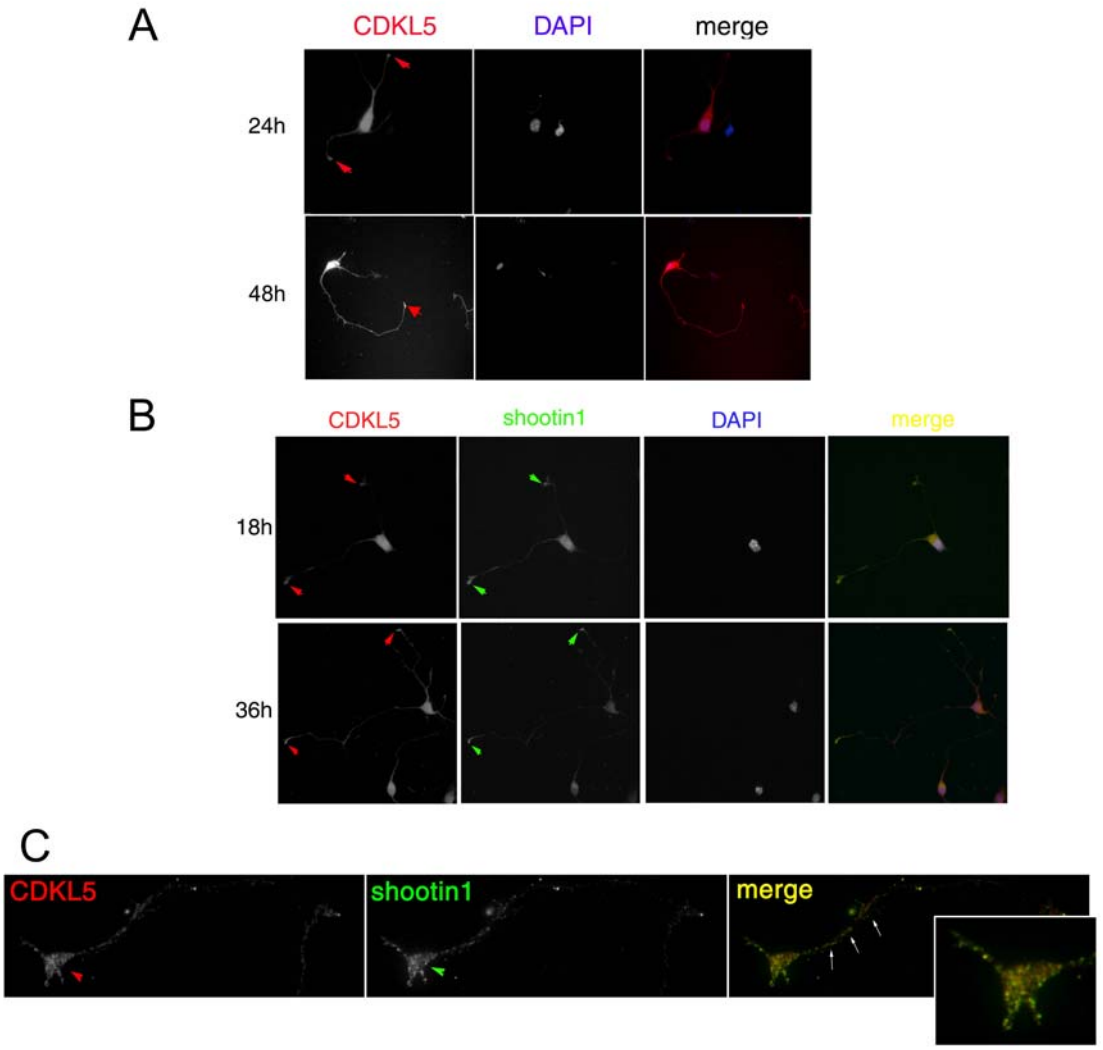


**FIGURE 10. CDKL5 accumulates in the axonal growth cone during in vitro neuronal polarization. A** Immunofluorescence experiments show CDKL5 expression and localization in primary hippocampal neurons at 24 h and 48 h after plating. Primary hippocampal neurons were prepared from E18 mouse embryos and the subcellular localization of endogenous CDKL5 (red) analyzed by indirect immunofluorescence. In the cell body CDKL5 is diffused and accumulates in the axonal growth cone (arrowheads). Nuclei were stained with DAPI (blue). **B** CDKL5 (red) and shootin1 (green) co-localize in primary hippocampal neurons at 18 h and 36 h. The overlap between the two proteins appears in yellow (merge). Images represent a 40X magnification. Nuclear staining with DAPI appears in blue. **C** Magnification of a growth cone that shows co-localization in the tip (arrowhead) but not along the neurite (arrows). The insert shows in details the axonal growth cone where a co-localization of the two proteins is evident (100X magnification).

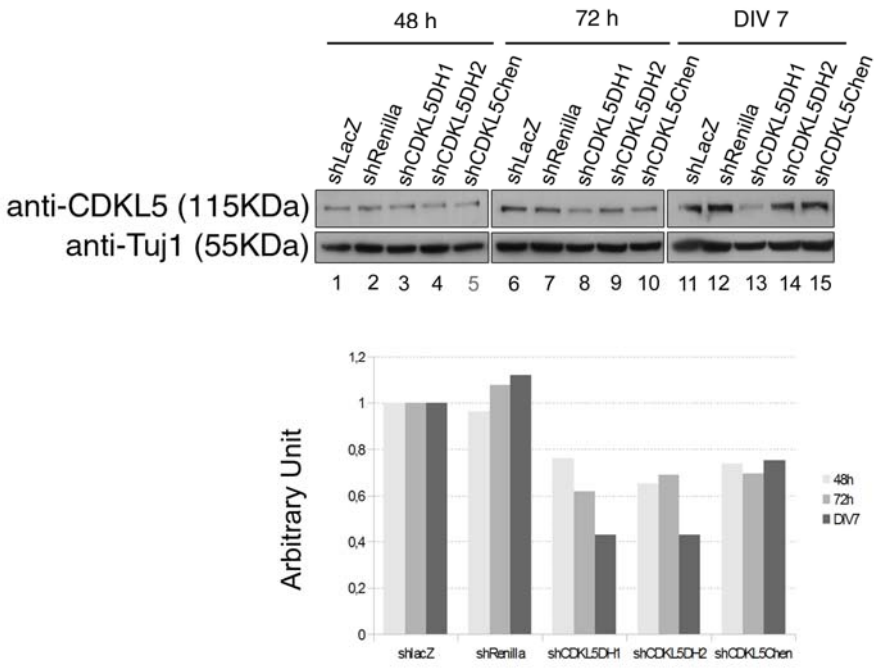


**FIGURE 11. Downregulation of CDKL5 in hippocampal neurons infected with lentiviral shRNA particles.** Western blotting analysis showing cultured hippocampal neurons interfered for CDKL5 at 48, 72 hours or DIV 7 (upper panel). Evaluation of ablation of CDKL5 (lower panel). CDKL5 levels were normalized to those of Tuj1 and the obtained values expressed as fold expression relative to the controls (shLacZ).

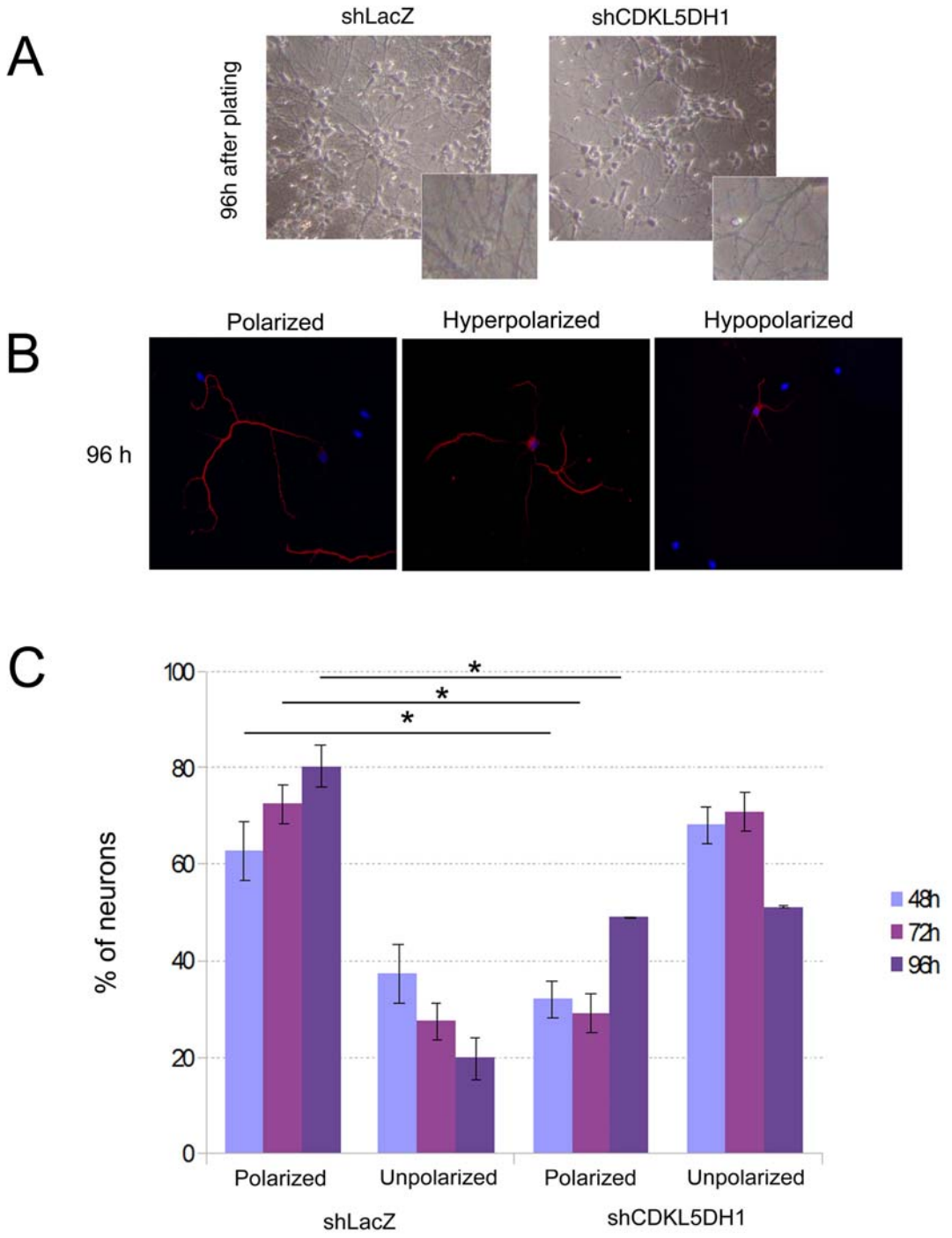


**FIGURE 12. CDKL5 knockdown affects neuronal development in cultured hippocampal neurons. A** Representative image of neurons infected for 96 h with shLacZ or shCDKL5DH1. The neuronal network (magnification) is reduced in interfered cells with respect to the control. **B** Representative images of hippocampal neurons, fixed at 96 h after plating, stained with the axonal marker Tau-1. Polarized neurons: 1-axon; hyperpolarized > 1-axon; hypopolarized: no axon. **C** Statistical analysis of loss-of-function experiments. Neurons were analyzed at 48, 72 and 96 h after plating and infection with shLacz or shCDKL5DH1. Data represent mean ± SEM; n= 109 – 144 in each group; *p>0.01; t test.

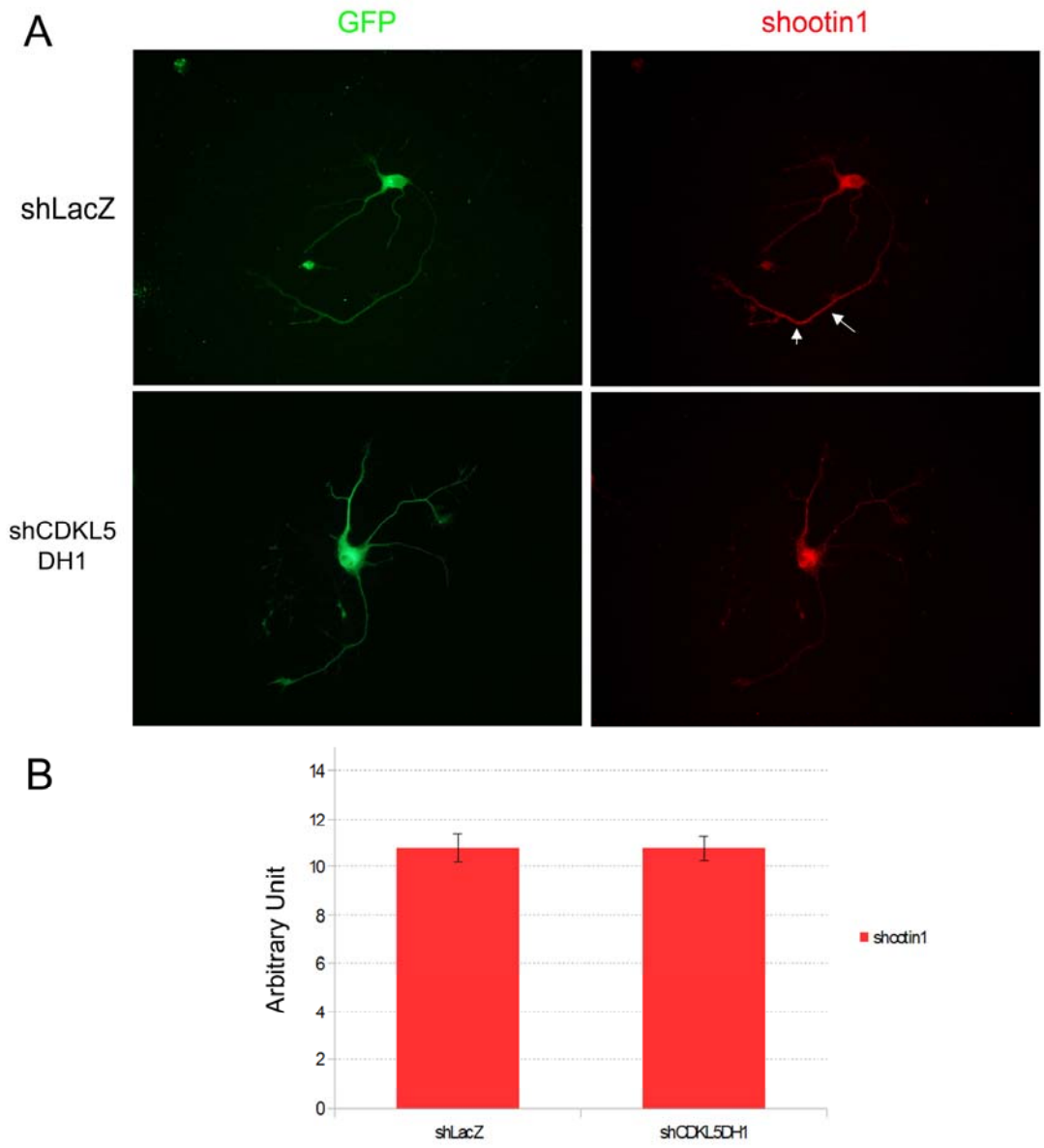


**FIGURE 13. Loss of CDKL5 affects shootin1 localization during the first stages of neuronal development. A** Hippocampal neurons infected with shLacZ or shCDKL5DH1 for 72 h were stained with anti-shootin1 (red). In shLacZ expressing control neurons shootin1 accumulated with a proximal to distal increase in staining intensity along the axon (white arrows), whereas in shCDKL5DH1 neurons shootin1 was diffuse in all neurites. **B** Statistical analysis showing shootin1 protein levels in control neurons and those silenced for CDKL5. The overall quantity of shootin1 is not reduced by silencing of CDKL5. Data represent mean ± SEM; n= 10 in each group.

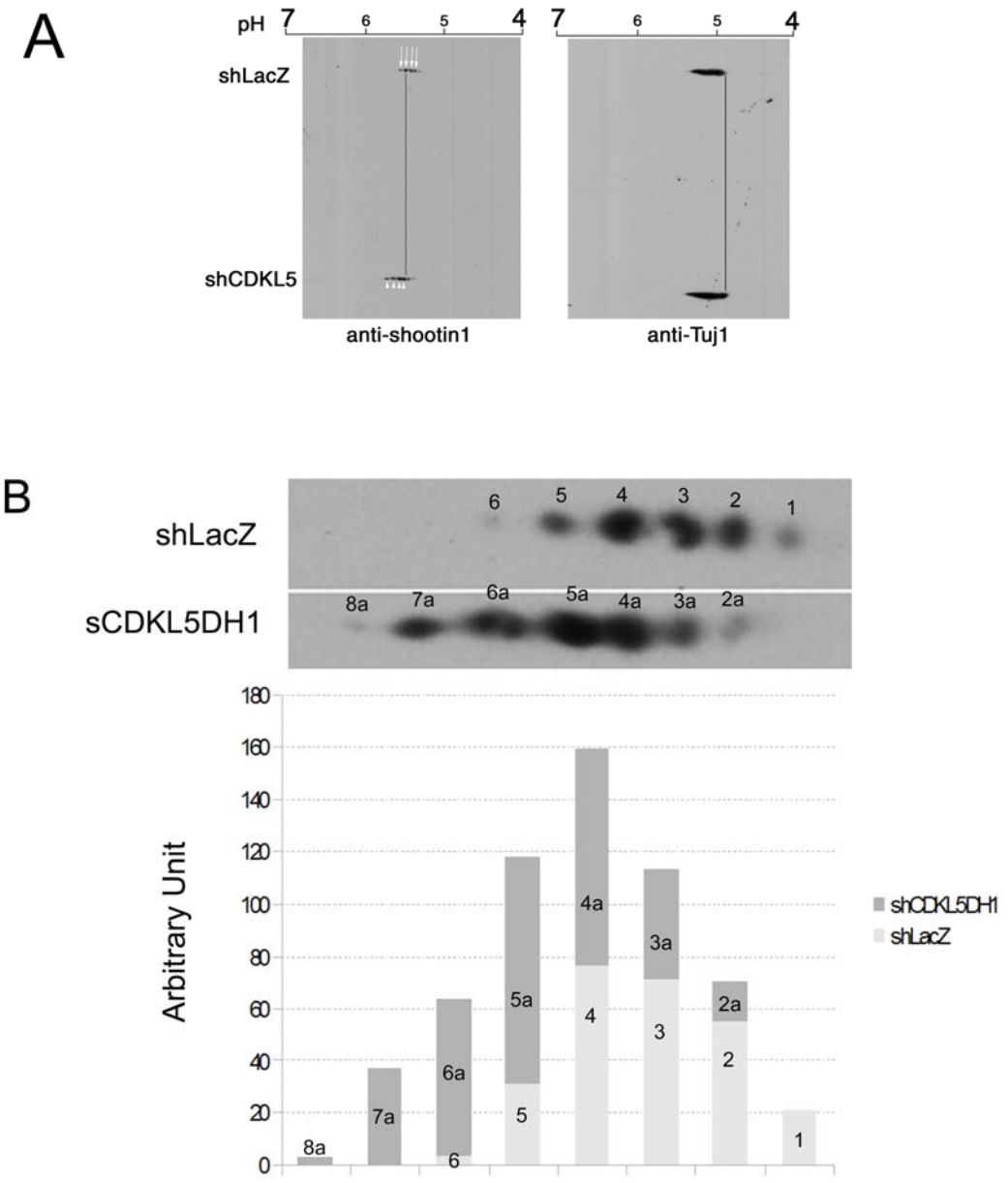


**FIGURE 14. Silencing of CDKL5 affects shootin1 phosphorylation in primary neurons. A** Shootin1 was analyzed by IEF followed by WB of total brain extracts of shRNA treated neurons. Tuj1 was used as internal standard to align the spots. **B** Magnification of the aligned shootin1 signals. In shCDKL5DH1 treated neurons the shootin1 isoforms are characterized by a more basic pH with respect to the control sample (shLacZ). The graf represents the quantification of the spots.

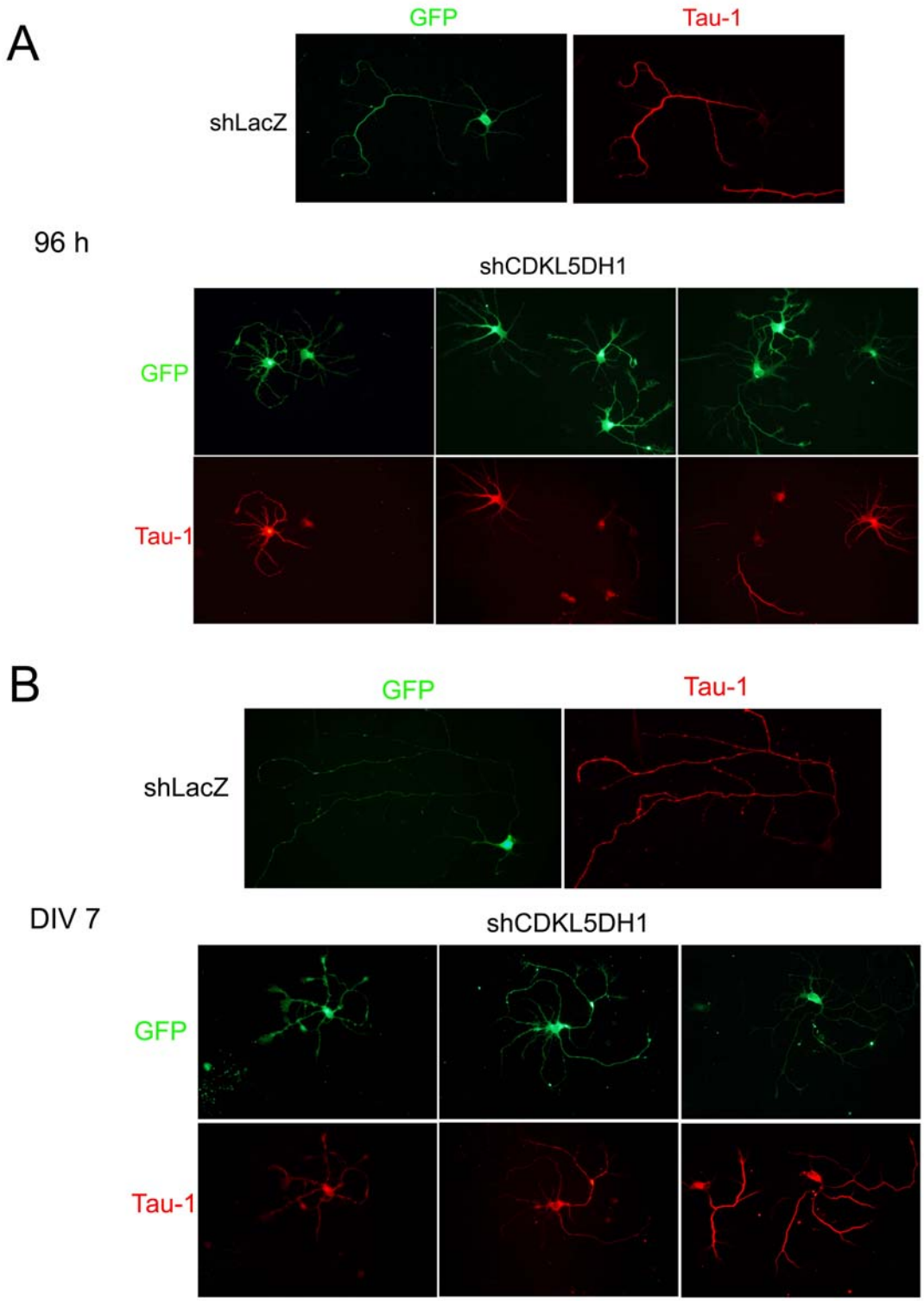


**FIGURE 15. CDKL5 silencing affects neuronal morphology. A – B** Hippocampal neurons were infected with shLacZ or shCDKL5DH1. For each maturation stage (96 h and DIV7) three representative neurons are shown. Neurons expressing plasmids are identified by GFP signal (green). Morphology of cells are analyzed considering GFP signal, and the axon are visulized by Tau-1 staining (red).

# DISCUSSION

Rett syndrome is a progressive neurodevelopment disorder affecting almost exclusively females. Its classical form is characterized by the appearance of symptoms after several months of apparently normal psyco-physical development followed by neurodevelopment arrest and regression (Hagberg et al. 1983): symptoms that appear during this period of infantile life will persist throughout the whole adulthood, preventing affected individuals from leading a normal and independent physical and social life. The classical form of RTT is mainly associated with mutations in the methyl-CpG binding protein 2 (MeCP2), identified as a transcriptional repressor, and more recently also proposed as an activator, involved in neurotrophin- and neuronal activity-mediated gene expression. Besides the classical form, also atypical cases of RTT have been reported: they are characterized both by milder phenotypes, as in the case of the “preserved speech variant”, and by more severe syndromes, such as the Hanefeld variant. Children affected by this variant, develop seizures soon after birth and the epileptic crisis often become pharmacologically intractable (Hanefeld et al. 1985). In accordance with the fact that less than 50% of RTT variants are caused by alterations in *MECP2*, mutations in the *CDKL5* gene have been identified in patients with the Hanefeld variant and other X-linked neurological syndromes (Rusconi et al. 2008): The involvement of CDKL5 in the aetiology of several neurodevelopmental disorders, including early-onset encephalopathy, infantile spasms and atypical RTT, underscores the importance of this protein for neuronal functions. However, its functions are far from being entirely understood, precluding an understanding of its role in the pathogenetic processes.

Here, we analyzed the functions of CDKL5 through the identification and characterization of its protein interactors. We decided to perform a yeast two-hybrid assay with an external service, Hybrigenics, using the C-terminal tail of CDKL5 (aa 299-1030) as bait to screen a human adult brain cDNA library. From this screen we obtained a list of 75 clones, considered probable interactors, from which four main pathways likely to involve CDKL5 could be evinced. One pathway regards neuronal polarization and includes four proteins (KIAA1598, FMNL2, GPRASP2, and GRLF1). In particular GRLF1, also called p190A, is a RhoGAP protein that constitutes the major inhibitor of Rho GTPases. Notably Chen et al., have recently demonstrated a link between CDKL5 and Rac1, a Rho GTPase involved in neuronal development. The second pathway includes the cytoskeleton with three proteins (DSP, DST, SPTBN1). Finally, pathways including neuronal transport with two proteins (KIF5A and NEFL) and cell signalling and degradation with five proteins (SPRY2, SPRED2, ASB3, KLHL7, UBE4A) could be extracted from the list. We focused our attention on the only interactor with the highest score, KIAA1598, included in the first hypothetical pathway. The gene KIAA1598, also called shootin1, encodes a protein with a key role in neuronal polarization and axonal specification (Toriyama et al. 2006). Shootin1 was identified few years ago in a proteomic analysis of axonal proteins that are upregulated during neuronal polarization. Accordingly, in a further characterization, its spatiotemporal localization in hippocampal neurons was found to change dynamically during polarization: it became upregulated, began fluctuating and building up in multiple neurites, and eventually accumulated asymmetrically in a single neurite. Shootin1 therefore has the prerequisites of providing the asymmetric signal for neuronal polarization and, accordingly, disturbing the asymmetric organization by excess or reduced levels of shootin1 multiple axons or inhibition of polarization are observed. In this context, we compared the expression pattern of CDKL5 and shootin1, and our results showed that, during development, the two proteins are present together between P4 and P14 post-natal stages. This was consistent with previous publications indicating that the *Cdkl5* mRNA is undetectable during prenatal development (Montini et al. 1998) and increases in early postnatal life reaching a peak of expression at P10 (Mari et al. 2005). Moreover, cellular fractionation analyses demonstrated that the kinase is present together with shootin1 in the cytosolic compartment in the early stages of development between E18 and P7. Taken together, these results suggested that the two proteins might interact early

in neuronal development and open the possibility of a new role of CDKL5 outside the nucleus and independent of MeCP2. By reciprocal co-immunoprecipitation experiments using total lysates from P7 mouse brains we were able to detect an interaction between endogenous CDKL5 and shootin1. In contrast, we could not detect any association when the exogenous proteins where purified from HEK293 cells, indicating that the interaction could be neuronal specific. In favour of a role of CDKL5 in the early stages of neuronal polarization we also observed that it accumulates in the distal tip of the neurites and co-localizes with shootin1 in the axonal growth cone 48 h after plating. Specific phosphorylation events have been found to regulate neuronal polarization and our data suggested that CDKL5 might belong to the group of kinases involved in this process. To verify our hypothesis, we approached loss-of-function experiments, where CDKL5 was silenced in primary hippocampal neurons using shRNA lentiviral vectors. Notably, we found that the ablation of CDKL5 has a dramatic effect on two aspects of neuronal maturation. First of all, neuronal network formation in interfered neurons is reduced with less processes extending from the cell bodies as already published by Chen et al. The authors quantified the total length of axons and dendrites and found a decrease of approximately 50% when CDKL5 was silenced in rat hippocampal neurons. This effect was found to be specific for the loss of CDKL5 since it could be prevented by co-expressing a shRNA-resistant from of CDKL5. However, in contrast to what was observed by Chen et al. we found that the loss of CDKL5 also causes a defect in neuronal polarization. Indeed, when we analyzed the establishment of neuronal polarity at 48, 72, 96 hours and at DIV7 by counting Tau1 positive processes the percentage of polarized control neurons increased from 63% at 48 h to 80% at 96 h. In contrast to that, the suppression of CDKL5 caused a reduction of the polarized phenotype so that only 32% and 29% of the cells were polarized at 48 and 72 h, respectively. At 96 h and at DIV7 we observed a slight recovery but found that still only approximately 50% of the neurons were characterized by one Tau1 positive process showing that the deficiency of CDKL5 causes a defect in neuronal polarization. Even if we did not show the specificity of CDKL5 by rescuing the phenotype with a shRNA resistant derivative of the kinase, we found that a second shRNA construct silencing CDKL5 to a lesser extent generated a similar but milder phenotype. This indicates that the observed effect on neuronal polarization is indeed a direct effect caused by the loss of CDKL5.

To directly test whether CDKL5 might be involved in neuronal polarization through shootin1, we checked its localization in hippocampal neurons, expressing shLacZ and shCDKL5DH1, at 72 h. At this time point, shootin1 still accumulates in the axon and the silencing of CDKL5 has already started. In control neurons, shootin1 appears normally localized in the axons with a significant increase in proximal to distal staining intensity, whereas in knock-down neurons, where the total levels of shootin1 remain unaltered, its accumulation in the axon disappears and the protein remains diffusely localized in the soma. Moreover, in 2D-IEF experiments the isoforms of shootin1 appeared more basic in the absence of CDKL5, according with the loss of one or more phosphate group(s), opening the possibility that shootin1 is a target of the catalytic activity of CDKL5. Taken together, these results indicate that CDKL5 may affect neuronal polarization in a shootin1-dependent manner, where CDKL5 is required for shootin1 to induce axon formation. Thus, we can hypotese that the reduced polarization observed after silencing of CDKL5 could be the consequence of lack of shootin1 in the growth cone. Toriyama et al. (2010) observed that shootin1 accumulates in the neurite tips in a neurite length-dependent manner. Through quantitative live cell imaging and modelling analyses, the authors revealed that intraneuritic anterograde transport and retrograde diffusion of shootin1 account for its neurite length-dependent accumulation. The role of CDKL5 might be that of phosphorylating shootin1 at the distal tip thereby allowing the protein to accumulate here or, alternatively, regulating the anterograde transport of shootin1 in a phosphorylation dependent manner. It would be interesting in the future to map the phosphorylation sites within shootin1 and assay the localization of its phospho-defective and –mimetic derivatives and their capacity to induce multiple axons.

It is important to mention, though, that in contrast to the data published by Toriyama et al. (2006), the silencing of CDKL5 has a stronger effect on axon formation since the polarization defect is not recovered at later stages of maturation as is the case with shootin1. In particular, when the maturation is complete, the cells have lost their asymmetric shape and are characterized by having shorter neurites than the control cells as described also by Chen et al. (2010). The observed effect on neuronal polarization observed upon ablation of CDKL5 might therefore also be due to a distruption of cytoskeleton. In fact, as mentioned above, shootin1 is transported from the cell body to the growth cones through an actin- and myosin-dependent mechanism and diffuses back to the cell body (Toriyama et al. 2006). If CDKL5 works

on cytoskeleton maintenance, disruption of actin or myosin cytoskeleton could prevent the active transport of shootin1 to the growth cones, with the consequence that the latter is not present where it is necessary for inducing axonal outgrowth. In this context, the effect of CDKL5 on shootin1 accumulation and phosphorylation might be indirect. Multiple post-transcriptional modifications such as phosphorylation have been implicated in the highly articulated processes of neuronal maturation. They involve a number of proteins and protein complexes, among which a particular role is played by the Rho-family. The well-established pathway of p21-activated kinase (PAK) activation via Cdc42 or Rac results in inhibition of the actin depolymerising factor cofilin by activating its inhibitor, LIM kinase (Dan et al. 2001). Other notable targets of PAK include the myosin activator, myosin light chain kinase (MLCK), and the microtubule destabilizating protein, Op18/stathmin, which are inhibited by PAK phosphorylation. The cytoskeleton is a main player of both neuronal shape and polarization and its disruption leads to alterations in neuronal morphology. As described by Chen et al., CDKL5 is involved in BDNF-Rac1 signaling. Rac1 is an important regulator of cell migration (Ridley, 2001), it is involved in axon growth as both a positive and negative regulator (Govek *et al.* 2005), and notably, it regulates both actin and microtubule dynamics (Kunda et al., 2001; Ng and Luo, 2004; Watabe-Uchida et al., 2006), with a particular involvement in axon formation through the actin cytoskeleton (Tahirovic et al. 2010).

Future experiments will be needed to elucidate the involvement of CDKL5 in regulating cytoskeleton manteinance. Regarding this, it might be useful to study other putative interactors found in the two-hybrid screening. For example, *SPTBN1* (spectrin beta, non-erythrocytic 1) might be interesting; it encodes an actin cross-linking and molecular scaffold protein linking the plasma membrane to the actin cytoskeleton and functions in the determination of cell shape, arrangement of transmembrane proteins, and organization of organelles (Hu et al. 1992). DST encoding dystonin, a member of the plakin protein family of adhesion junction plaque proteins, is another interesting interactor. Some of its isoforms are expressed in neuronal and muscle tissues, anchoring neural intermediate filaments to the actin cytoskeleton. Consistent with the expression profile, mice defective for dystonin show skin blistering and neurodegeneration (Young et al. 2008).

To conclude, we have identified a hitherto unknown role of CDKL5 in regulating neuronal polarization. This process is tightly linked to neuronal migration in vivo in

accordance with the data published by Chen et al. showing that neurons devoid of CDKL5 are characterized by a delay in migration. Importantly, disorders associated with defects in neuronal migration are characterized by intractable epilepsy and intellectual disability (Liu et al. 2011). In particular, many of these genes are involved in cytoskeleton regulation including the function of microtubules and of actin. Thus, defects observed in the maintenance of cytoskeleton due to CDKL5 ablation could recapitulate the symptoms of the Hanefeld variant characterized by a epileptic seizure often farmacologically intractable. It will therefore be interesting in the future, when appropriate *Cdkl5* mouse models are available, to understand what are the developmental consequences of the lack of CDKL5.

# BIBLIOGRAPHY

**Adler DA**, Quaderi NA, Brown SD, Chapman VM, Moore J, Tate P, Disteche CM. The X-linked methylated DNA binding protein, Mecp2, is subject to X inactivation in the mouse. Mamm Genome Aug;6(8):491-2 (1995).

**Amir RE**, Fang P, Yu Z, Glaze DG, Percy AK, Zoghbi HY, Roa BB, Van den Veyver IB Mutations in exon 1 of MECP2 are a rare cause of Rett syndrome. J Med Genet Feb;42(2):e15 (2005).

**Archer HL**, Evans JC, Millar DS, Thompson PW, Kerr AM, Leonard H, Christodoulou J, Ravine D, Lazarou L, Grove L, Verity C, Whatley SD, Pilz DT, Sampson JR, Clarke AJ NTNG1 mutations are a rare cause of Rett syndrome. Am J Med Genet A. Apr 1;140(7):691-4 (2006).

**Archer HL**, Evans J, Edwards S, Colley J, Newbury-Ecob R, O'Callaghan F, Huyton M, O'Regan M, Tolmie J, Sampson J, Clarke A, Osborne J. CDKL5 mutations cause infantile spasms, early onset seizures, and severe mental retardation in female patients. J Med Genet Sep;43(9):729-34 (2006).

**Armstrong DD**, Dunn JK, Antalffy B, Trivedi R. Selective dendritic alteratins in the cortex of Rett synfrome. J Neuropathol Exp Neurol; 54:195-201 (1995).

**Bahi-Buisson N**, Kaminska A, Boddaert N, Rio M, Afenjar A, Gérard M, Giuliano F, Motte J, Héron D, Morel MA, Plouin P, Richelme C, des Portes V, Dulac O, Philippe C, Chiron C, Nabbout R, Bienvenu T. The three stages of epilepsy in patients with CDKL5 mutations. Epilepsia Jun;49(6):1027-37 (2008).

**Bahi-Buisson N**, Nectoux J, Rosas-Vargas H, Milh M, Boddaert N, Girard B, Cances C, Ville D, Afenjar A, Rio M, Héron D, N'guyen Morel MA, Arzimanoglou A, Philippe C, Jonveaux P, Chelly J, Bienvenu T. Key clinical features to identify girls with CDKL5 mutations. Brain Oct;131(Pt 10):2647-61 (2008).

**Bertani I**, Rusconi L, Bolognese F, Forlani G, Conca B, De Monte L, Badaracco G, Landsberger N, Kilstrup-Nielsen C. Functional consequences of mutations in CDKL5, an X-linked gene involved in infantile spasms and mental retardation. J Biol Chem 281:32048-32056 (2006).

**Bracaglia G**, Conca B, Bergo A, Rusconi L, Zhou Z, Greenberg ME, Landsberger N, Soddu S, Kilstrup-Nielsen C. Methyl-CpG-binding protein 2 is phosphorylated by homeodomain-interacting protein kinase 2 and contributes to apoptosis. EMBO Rep Dec;10(12):1327-33 (2009).

**Bradke F** and Dotti CG. The role of local actin instability in axon formation. Science 283;1931-1934 (1999).

**Budden SS**. Management of Rett sindrome: a ten year experience. Neuropediatrics. 1995 Apr;26(2):75-7.

**Budden SS**. Rett sindrome: habilitation and management reviewed. Eur Child Adolesc Psychiatry. 1997;6 Suppl 1:103-7. Review.

**Calzado MA**, Renner F, Roscic A, Schmitz ML. HIPK2: a versatile switchboard regulating the transcription machinery and cell death. Cell Cycle Jan 15;6(2):139-43 Review (2007).

**Chahrour M**, Zoghbi HY. The story of Rett syndrome: from clinic to neurobiology. Neuron Nov 8;56(3):422-37. Review (2007).

**Chao HT**, Zoghbi HY. The yin and yang of MeCP2 phosphorylation. Proc Natl Acad Sci U S A Mar 24;106(12):4577-8 (2009).

**Chen Q**, Zho YC, Yu J, Miao S, Zheng J, Xu l, Zhou Y, Li D, Zhang C, Tao J, Xiong ZQ. CDKL5, a protein associated with Rett sindrome, regulates neuronal morpholgenesis via Rac1 signaling. The J of Neur 9 22,30(38):12777-12786 (2010).

**Chen RZ**, Akbarian S, Tudor M, Jaenisch R. Deficiency of methyl-CpG binding protein-2 in CNS neurons results in a Rett-like phenotype in mice. Nat Genet Mar;27(3):327-31 (2001).

**Chen WG**, Chang Q, Lin Y, Meissner A, West AE, Griffith EC, Jaenisch R, Greenberg ME. Derepression of BDNF transcription involves calcium-dependent phosphorylation of MeCP2. Science Oct 31;302(5646):885-9 (2003).

**Christodoulou J**, Grimm A, Maher T, Bennetts B. RettBASE: The IRSA MECP2 variation database-a new mutation database in evolution. Hum Mutat May;21(5):466-72 (2003).

**Chung AS**, Guan YJ, Yuan ZL, Albina JE, Chin YE. Ankyrin repeat and SOCS box 3 (ASB3) mediates ubiquitination and degradation of tumor necrosis factor receptor II. Mol Cell Biol Jun;25(11):4716-26 (2005).

**Collins AL**, Levenson JM, Vilaythong AP, Richman R, Armstrong DL, Noebels JL, David Sweatt J, Zoghbi HY. Mild overexpression of MeCP2 causes a progressive neurological disorder in mice. Hum Mol Genet Nov 1;13(21):2679-89 (2004).

**Contino G**, Amati F, Pucci S, Pontieri E, Pichiorri F, Novelli A, Botta A, Mango R, Nardone AM, Sangiuolo FC, Citro G, Spagnoli LG, Novelli G. Expression analysis of the gene encoding for the U-box-type ubiquitin ligase UBE4A in human tissues. Gene Mar 17;328:69-74 (2004).

**Cowan CR**, and Hyman AA. Asymmetric cell division in C.elegans: cortical polarity and spindle positioning. Annu. Rev. Cell Dev. Biol., 20;427-453 (2004).

**Dan C**, Kelly A, Bernard O, Minden A. Cytoskeletal changes regulated by the PAK4 serine/threonine kinase are mediated by LIM kinase 1 and cofilin. J Niol Chem; Aug 24;276(34):32115-21 (2001).

**Dayer AG**, Bottani A, Bouchardy I, Fluss J, Antonarakis SE, Haenggeli CA, Morris MA. MECP2 mutant allele in a boy with Rett syndrome and his unaffected heterozygous mother. Brain Dev Jan;29(1):47-50 (2007).

**Dotti CG**, Sullivan CA and Banker GA. The establishment of polarity by hippocampal neurons in culture. J. Neurosci 8;1454-1468 (1988).

**Dragich JM**, Kim YH, Arnold AP, Schanen NC. Differential distribution of the MeCP2 splice variants in the postnatal mouse brain. J Comp Neurol. Apr 1;501(4):526-42 (2007).

**Egger J**, Hofacker N, Schiel W, Holthausen H. Magnesium for hyperventilation in Rett's syndrome. Lancet Sep 5;340(8819):621-2 (1992).

**Ellaway CJ**, Badawi N, Raffaele L, Christodoulou J, Leonard H. A case of multiple congenital anomalies in association with Rett syndrome confirmed by MECP2 mutation screening. Clin Dysmorphol Jul;10(3):185-8 (2001).

**Etemad-Moghadam B**, Guo S and Kemphues KJ. Asymmetrically distributed PAR-3 protein contributes to cell polarity and spindle alignment in early *C.elegans* embryo. Cell 83;743-752 (1995).

**Evans JC**, Archer HL, Colley JP, Ravn K, Nielsen JB, Kerr A, Williams E, Christodoulou J, Gécz J, Jardine PE, Wright MJ, Pilz DT, Lazarou L, Cooper DN, Sampson JR, Butler R, Whatley SD, Clarke AJ. Early onset seizures and Rett-like features associated with mutations in CDKL5. Eur J Hum Genet Oct;13(10):1113-20 (2005).

**Fichou Y**, Nectoux J, Bahi-Buisson N, Chelly J, Bienvenu T. An isoform of the severe encephalopathy-related CDKL5 gene, including a novel exon with extremely high sequence conservation, is specifically expressed in brain. J Hum Genet Jan;56(1):52-57 (2011).

**Fukata A**, Kimura T and Kaibuchi K. Axon specification in hippocampal neurons. Neurosci. Res 43;305-315 (2002).

**Gou S**, and Kemphues KJ. par-1, a gene required for establishing polarity in *C.elegans* embryos, encodes a putatie Ser/Thr kinase that is asymmetrically distributed. Cell 81;611-620 (1995).

**Govek EE,** Newey SE, Van Aelst L. The role of the Rgo GTPase in neuronal development. Genes Dev;19:1-49 (2005).

**Grosso S**, Brogna A, Bazzotti S, Renieri A, Morgese G, Balestri P. Seizures and electroencephalographic findings in CDKL5 mutations: case report and review. Brain Dev May;29(4):239-42 (2007).

**Guy J**, Hendrich B, Holmes M, Martin JE, Bird A. A mouse Mecp2-null mutation causes neurological symptoms that mimic Rett syndrome. Nat Genet Mar;27(3):322-6 (2001).

**Guy J**, Gan J, Selfridge J, Cobb S, Bird A. Reversal of neurological defects in a mouse model of Rett syndrome. Science Feb 23;315(5815):1143-7 (2007).

**Hagberg B**, Aicardi J, Dias K, Ramos O. A progressive syndrome of autism, dementia, ataxia, and loss of purposeful hand use in girls: Rett syndrome: report of 35 cases. Ann Neurol (1983).

**Hagberg B**, Hanefeld F, Percy A, Skjeldal O. An update on clinically applicable diagnostic criteria in Rett syndrome. Eur J Paediatr Neurol 6(5):293-7 (2002).

**Hanefeld F**. The clinical pattern of the Rett syndrome. Brain Dev 7(3):320-5 (1985).

**Harikrishnan KN**, Chow MZ, Baker EK, Pal S, Bassal S, Brasacchio D, Wang L, Craig JM, Jones PL, Sif S, El-Osta A. Brahma links the SWI/SNF chromatin-remodeling complex with MeCP2-dependent transcriptional silencing. Nat Genet. Mar;37(3):254-64 (2005).

**Horn SC**, Lalowski M, Goehler H, Dröge A, Wanker EE, Stelzl U. Huntingtin interacts with the receptor sorting family protein GASP2. J Neural Transm Aug;113(8):1081-90 (2006).

**Horton AC** and Ehlers MD. Neuronal polarity and trafficking. Neuron 40;277-295 (2003).

**Hu RJ**, Watanabe M, Bennett V. Characterization of human brain cDNA encoding the general isoform of beta-spectrin. J Biol Chem. Sep 15;267(26):18715-22 (1992).

**Hung TJ** and Kemphues KJ. PAR-6 is a conserved PDZ domain-containing protein that colocalizes with PAR-3 in *Caenorhabditis elegans* embryos. Development,126;127-135 (1999).

**Huopaniemi L**, Tyynismaa H, Rantala A, Rosenberg T, Alitalo T. Characterization of two unusual RS1 gene deletions segregating in Danish retinoschisis families. Hum Mutat Oct;16(4):307-14 (2000).

**Jellinger K**, Seitelberger F. Neuropathology of Rett syndrome. Am J Med Genet Suppl 1:259-88 (1986).

**Jones PL**, Veenstra GJ, Wade PA, Vermaak D, Kass SU, Landsberger N, Strouboulis J, Wolffe AP. Methylated DNA and MeCP2 recruit histone deacetylase to repress transcription. Nat Genet Jun;19(2):187-91 (1998).

**Kalscheuer VM**, Tao J, Donnelly A, Hollway G, Schwinger E, Kübart S, Menzel C, Hoeltzenbein M, Tommerup N, Eyre H, Harbord M, Haan E, Sutherland GR, Ropers HH, Gécz J. Disruption of the serine/threonine kinase 9 gene causes severe X-linked infantile spasms and mental retardation. Am J Hum Genet Jun;72(6):1401-11 (2003).

**Kameshita I**, Sekiguchi M, Hamasaki D, Sugiyama Y, Hatano N, Suetake I, Tajima S and Sueyoshi N. Cyclin-dependent kinase-like 5 binds and phosphorylates DNA methyltransferase 1. Bioch.and Biop.Res. Comm 377;1162-1167 (2008).

**Kerr AM**, Nomura Y, Armstrong D, Anvret M, Belichenko PV, Budden S, Cass H, Christodoulou J, Clarke A, Ellaway C, d'Esposito M, Francke U, Hulten M, Julu P, Leonard H, Naidu S, Schanen C, Webb T, Engerstrom IW, Yamashita Y, Segawa M. Guidelines for reporting clinical features in cases with MECP2 mutations. Brain Dev Jul;23(4):208-11 (2001).

**Klose RJ**, Sarraf SA, Schmiedeberg L, McDermott SM, Stancheva I, Bird AP. DNA binding selectivity of MeCP2 due to a requirement for A/T sequences adjacent to methyl-CpG. Mol Cell Sep 2;19(5):667-78 (2005).

**Kunda P**, Paganini G, Quiroga S, Kosik K, Caceres A. Evidence for the involvement of Tiam1 in axon formation. J. Neurosi;21:2361-2372 (2001).

**Lemmon V**, Farr K L, Lagenaur C. L1-mediated axon outgrowth occurs via a homophilic binding mechanism. Neuron 2:1597-1603 (1989).

**Levitan DJ**, Boyd L, Mello CC, Kemphues KJ and Stinchcomb DT. par-2, a gene required for blastomere asymmetry in *Caenorhabditis elegans*, encodes zinc-finger and ATP-binding motifs. Proc. Natl. Acad. Sci. USA 91; 6108-6112 (1994).

**Lin C**, Franco B, Rosner MR. CDKL5/Stk9 kinase inactivation is associated with neuronal developmental disorders. Hum Mol Genet Dec 15;14(24):3775-86 (2005).

**Liu J.S.** Molecular genetics of Neuronal Migration. Curr Neurol Neurosi Rep 11:171-178. (2011).

**Luikenhuis S**, Giacometti E, Beard CF, Jaenisch R. Expression of MeCP2 in postmitotic neurons rescues Rett syndrome in mice. Proc Natl Acad Sci U S A Apr 20;101(16):6033-8 (2004).

**Lybaek H**, Ørstavik KH, Prescott T, Hovland R, Breilid H, Stansberg C, Steen VM, Houge G. An 8.9 Mb 19p13 duplication associated with precocious puberty and a sporadic 3.9 Mb 2q23.3q24.1 deletion containing NR4A2 in mentally retarded members of a family with an intrachromosomal 19p-into-19q between-arm insertion. Eur J Hum Genet Jul;17(7):904-10 (2009).

**Matheson SF**, Hu KQ, Brouns MR, Sordella R, VanderHeide JD, Settleman J. Distrinct but overlapping functions for the closely related p19 RhoGAPs in neural development. Dev Neurosci;28(6):538-50 (2006).

**Mari F**, Azimonti S, Bertani I, Bolognese F, Colombo E, Caselli R, Scala E, Longo I, Grosso S, Pescucci C, Ariani F, Hayek G, Balestri P, Bergo A, Badaracco G, Zappella M, Broccoli V, Renieri A, Kilstrup-Nielsen C, Landsberger N. CDKL5 belongs to the same molecular pathway of MeCP2 and it is responsible for the early-onset seizure variant of Rett syndrome. Hum Mol Genet Jul 15;14(14):1935-46 (2005).

**McGraw CM**, Samaco RC, Zoghbi HY. Adult neural function requires MeCP2. Science Jul 8;333(6039):186 (2011).

**Montini E**, Andolfi G, Caruso A, Buchner G, Walpole SM, Mariani M, Consalez G, Trump D, Ballabio A, Franco B. Identification and characterization of a novel serine-threonine kinase gene from the Xp22 region. Genomics Aug 1;51(3):427-33 (1998).

**Morton DG**, Shankes DC, Nugent S, Dichoso D, Wang W,Golden A and Kemphues KJ, The Caenorhabditis elegans par-5 gene encodes a 14-3-3 protein required for cellular asymmetry in the early embryo. Dev Biol 241;47-58 (2002).

**Nan X**, Ng HH, Johnson CA, Laherty CD, Turner BM, Eisenman RN, Bird A. Transcriptional repression by the methyl-CpG-binding protein MeCP2 involves a histone deacetylase complex. Nature May 28;393(6683):386-9 (1998).

**Nectoux J**, Heron D, Tallot M, Chelly J, Bienvenu T. Maternal origin of a novel C-terminal truncation mutation in CDKL5 causing a severe atypical form of Rett syndrome. Clin Genet Jul;70(1):29-33 (2006).

**Nemos C**, Lambert L, Giuliano F, Doray B, Roubertie A, Goldenberg A, Delobel B, Layet V, N'guyen MA, Saunier A, Verneau F, Jonveaux P, Philippe C. Mutational spectrum of CDKL5 in early-onset encephalopathies: a study of a large collection of French patients and review of the literature. Clin Genet Oct;76(4):357-71 Review (2009).

**Neul JL**, Kaufmann WE, Glaze DG, Christodoulou J, Clarke AJ, Bahi-Buisson N, Leonard H, Bailey ME, Schanen NC, Zappella M, Renieri A, Huppke P, Percy AK; RettSearch Consortium. Rett syndrome: revised diagnostic criteria and nomenclature. Ann Neurol Dec;68(6):944-50 (2010).

**Ng J**, Luo L. Rho GTPases regulate axon growth through convergent and divergent signaling pathways. Neuron;44:779-793 (2004).

**Nikitina T**, Shi X, Ghosh RP, Horowitz-Scherer RA, Hansen JC, Woodcock CL. Multiple modes of interaction between the methylated DNA binding protein MeCP2 and chromatin. Mol Cell Biol.Feb;27(3):864-77 (2007).

**Nomura Y**, Segawa M, Hasegawa M. Rett syndrome--clinical studies and pathophysiological consideration. Brain Dev 6(5):475-86 (1984).

**Nomura Y**, Segawa M. Clinical features of the early stage of the Rett syndrome. Brain Dev 12(1):16-9 (1990).

**Nomura Y**, Segawa M. Natural history of Rett syndrome. J Child Neurol Sep;20(9):764-8. Review (2005).

**Nonami A**, Kato R, Taniguchi K, Yoshiga D, Taketomi T, Fukuyama S, Harada M, Sasaki A, Yoshimura A. Spred-1 negatively regulates interleukin-3-mediated ERK/mitogen-activated protein (MAP) kinase activation in hematopoietic cells. J Biol Chem Dec 10;279(50):52543-51 (2004).

**Psoni S**, Willems PJ, Kanavakis E, Mavrou A, Frissyra H, Traeger-Synodinos J, Sofokleous C, Makrythanassis P, Kitsiou-Tzeli S. A novel p.Arg970X mutation in the last exon of the CDKL5 gene resulting in late-onset seizure disorder. Eur J Paediatr Neurol Mar;14(2):188-91 (2010).

**Rademacher N**, Hambrock M, Fischer U, Moser B, Ceulemans B, Lieb W, Boor R, Stefanova I, Gillessen-Kaesbach G, Runge C, Korenke GC, Spranger S, Laccone F, Tzschach A, Kalscheuer VM. Identification of a novel CDKL5 exon and pathogenic mutations in patients with severe mental retardation, early-onset seizures and Rett-like features. Neurogenetics Feb 12 (2011).

**Reichardt LF**. Neurotrophin-regulated signaling pathways. Philos Trans R Soc Lond B Biol Sci 361:1545-1564 (2006).

**Reilly MM**. NEFL-related Charcot-Marie-tooth disease: an unraveling story. Ann Neurol Dec;66(6):714-6 (2009).

**Ricciardi S**, Kiltrup-Nielsen C, Bienvenu T, Jaquette A, Landsberger N, Broccoli V. CDKL5 influence RNA splicing activity by its association to the nuclear speckle molecular machinery. Hum Mol Gent 18(23):4590-4602 (2009).

**Ridley** AJ, Allen WE, Peppelenbosch M, Jones GE. Rho family proteins and cell migration. Biochem Soc Symp;65:111-23 (1999).

**Rinaldo C**, Prodosmo A, Siepi F, Soddu S. HIPK2: a multitalented partner for transcription factors in DNA damage response and development. Biochem Cell Biol Aug;85(4):411-8. Review (2007).

**Rosas-Vargas H**, Bahi-Buisson N, Philippe C, Nectoux J, Girard B, N'Guyen Morel MA, Gitiaux C, Lazaro L, Odent S, Jonveaux P, Chelly J, Bienvenu T. Impaiment of CDKL5 nuclear localisation as a cause for severe infantile encephalopaty. J Med Genet (2008).

**Rusconi L**, Salvatoni L, Giudici L, Bertani I, Kilstrup-Nielsen C, Broccoli V, Landsberger N.CDKL5 expression is modulated during neuronal development and its subcellular distribution is tightly regulated by the C-terminal tail. J Biol Chem Oct 31;283(44):30101-11 (2008).

**Sakiyama T**, Fujita H, Tsubouchi H. Autoantibodies against ubiquitination factor E4A (UBE4A) are associated with severity of Crohn's disease. Inflamm Bowel Dis. Mar;14(3):310-7 (2008).

**Scala E**, Ariani F, Mari F, Caselli R, Pescucci C, Longo I, Meloni I, Giachino D, Bruttini M, Hayek G, Zappella M, Renieri A. CDKL5/STK9 is mutated in Rett syndrome variant with infantile spasms. J Med Genet Feb;42(2):103-7 (2005).

**Shahbazian M**, Young J, Yuva-Paylor L, Spencer C, Antalffy B, Noebels J, Armstrong D, Paylor R, Zoghbi H. Mice with truncated MeCP2 recapitulate many Rett syndrome features and display hyperacetylation of histone H3. Neuron Jul 18;35(2):243-54 (2002).

**Sirianni N**, Naidu S, Pereira J, Pillotto RF, Hoffman EP. Rett syndrome: confirmation of X-linked dominant inheritance, and localization of the gene to Xq28. Am J Hum Genet Nov;63(5):1552-8 (1998).

**Shi SH**, Jan LY, Jan YN. Hippocampal neuronal polarity specified by spatially localized mPar3/mPar6 and PI3-kinase activity. Cell 112:63-75 (2003).

**Shimada T**, Toriyama M, Uemura K, Kamiguchi H, Sugiura T, Watanabe N and Inagaki N. Shootin1 interacts with actin retrograde flow and L1-CAM to promote axon outgrowth. J. Cell Biol 181;817-829 (2008).

**Tahirovic S**, Hellal F, Neukirchen D, Hindges R, Garvalov BK, Flynn KC, Stradal TE, Chrostek-Grashoff A, Brakebusch C, Bradke F. Rac1 regulates neuronal polarization through the WAVE complex. J Neurosci. May 19;30(20):6930-43 (2010).

**Tao J**, Van Esch H, Hagedorn-Greiwe M, Hoffmann K, Moser B, Raynaud M, Sperner J, Fryns JP, Schwinger E, Gécz J, Ropers HH, Kalscheuer VM. Mutations in the X-linked cyclin-dependent kinase-like 5 (CDKL5/STK9) gene are associated with severe neurodevelopmental retardation. Am J Hum Genet Dec;75(6):1149-54 (2004).

**Tao J**, Hu K, Chang Q, Wu H, Sherman NE, Martinowich K, Klose RJ, Schanen C, Jaenisch R, Wang W, Sun YE. Phosphorylation of MeCP2 at Serine 80 regulates its chromatin association and neurological function. Proc Natl Acad Sci U S A Mar 24;106(12):4882-7 (2009).

**Tessa A,** Silvestri G, de Leva MF, Modoni A, Denora PS, Masciullo M, Dotti MT, Casali C, Melone MA, Federico A, Filla A, Santorelli FM A novel KIF5A/SPG10 mutation in spastic paraplegia associated with axonal neuropathy. J Neurol Jul;255(7):1090-2 (2008).

**Tomar A**, Lim ST, Lim Y, Schlaepfer DD A FAK-p120RasGAP-p190RhoGAP complex regulates polarity in migrating cells. J Cell Sci Aug 15;122(Pt 16):3005 (2009).

**Toriyama M**, Shimada T, Kim KB, Mitsuba M, Nomura E, Katsuta K, Sakumara Y, Roepstorff P and Inagaki N. Shootin1: a protein involved in the organization of an asymmetric signal for neuronal polarization. J. Cell Biol 175;Oct 9;147-157 (2006).

**Uzumcu A**, Norgett EE, Dindar A, Uyguner O, Nisli K, Kayserili H, Sahin SE, Dupont E, Severs NJ, Leigh IM, Yuksel-Apak M, Kelsell DP, Wollnik B. Loss of desmoplakin isoform I causes early onset cardiomyopathy and heart failure in a Naxos-like syndrome. J Med Genet Feb;43(2):e5 (2006).

**Watts** JL, Morton DG, Bestman J, Kemphues KJ. The *C-elegans* par-4 gene encodes a putative serine-threonine kinase required for establishing embryonic asymmetry. DevelopmentApr;127(7):1467-75 (2000).

**Weaving LS**, Ellaway CJ, Gécz J, Christodoulou J. Rett syndrome: clinical review and genetic update. J Med Genet Jan;42(1):1-7. Review (2005).

**Weaving LS**, Christodoulou J, Williamson SL, Friend KL, McKenzie OL, Archer H, Evans J, Clarke A, Pelka GJ, Tam PP, Watson C, Lahooti H, Ellaway CJ, Bennetts B, Leonard H, Gécz J. Mutations of CDKL5 cause a severe neurodevelopmental disorder with infantile spasms and mental retardation. Am J Hum Genet Dec;75(6):1079-93 (2004).

**Webb T**, Clarke A, Hanefeld F, Pereira JL, Rosenbloom L, Woods CG Linkage analysis in Rett syndrome families suggests that there may be a critical region at Xq28. J Med Genet Dec;35(12):997-1003 (1998).

**Williamson SL**, Giudici L, Kilstrup-Nielsen C, Gold W, Pelka GJ, Tam PP, Grimm A Prodi D, Landsberger N, Christodoulou J. A novel transcript of cyclin-dependent kinase-like 5 (CDKL5) has an alternative C-terminus and is the predominant transcript in brain. Hum Genet;jul 12 (2011).

**Witt-Engerström I**. Rett syndrome: The late infantile regression period-A retrospettive analysis of 91 cases. Acta Paediatr;81:167-172 (1992a).

**Witt Engerström I**. Age-related occurrence of signs and symptoms in the Rett syndrome. Brain Dev May;14 Suppl:S11-20 (1992b).

**Xiang F**, Zhang Z, Clarke A, Joseluiz P, Sakkubai N, Sarojini B, Delozier-Blanchet CD, Hansmann I, Edström L, Anvret M. Chromosome mapping of Rett syndrome: a likely candidate region on the telomere of Xq. J Med Genet Apr;35(4):297-300 (1998).

**Young KG**, Kothary R.Dystonin/Bpag1 is a necessary endoplasmic reticulum/nuclear envelope protein in sensory neurons. Exp Cell Res. Sep 10;314(15):2750-61 (2008).

**Yusoff P**, Lao DH, Ong SH, Wong ES, Lim J, Lo TL, Leong HF, Fong CW, Guy GR. Sprouty2 inhibits the Ras/MAP kinase pathway by inhibiting the activation of Raf.
J Biol Chem Feb 1;277(5):3195-201 (2002).

**Zhou Z**, Hong EJ, Cohen S, Zhao WN, Ho HY, Schmidt L, Chen WG, Lin Y, Savner E, Griffith EC, Hu L, Steen JA, Weitz CJ, Greenberg ME. Brain-specific phosphorylation of MeCP2 regulates activity-dependent Bdnf transcription, dendritic growth, and spine maturation. Neuron Oct 19;52(2):255-69 (2006).